Original Article

Monilinia fructicola as a Driver of Fungal Dysbiosis and Microbial Network Disruption in *Prunus persica*

Baltazar E.[1], Leitão R.[1], Rodrigues S.[1,2], Figueira D.[1,2]; Garcia E.[1,2], Costa J.[1,2*]

[1]University of Coimbra - Center for Functional Ecology Science for People & the Planet, TERRA Associated Laboratory, Department of Life Sciences, Calçada Martim de Freitas, Coimbra 3000-456, Portugal.

[2]Laboratory for Phytopathology, Instituto Pedro Nunes, R. Pedro Nunes, 3030-199 Coimbra, Portugal

* Corresponding author: Joana Costa; jcosta@uc.pt

Abstract

Fungal community dynamics play a fundamental role in plant health, influencing resilience, disease progression, and ecosystem stability. *Monilinia fructicola*, a quarantine pathogen affecting *Prunus persica*, is hypothesized to drive fungal dysbiosis by altering microbial diversity, ecological interactions and functional roles. In this study, its impact on fungal community composition, trophic dynamics, and network structure was investigated using ITS metabarcoding and high-throughput sequencing of flowers and branches from infected and non-infected *P. persica* trees were analysed. Results showed a pathogen-induced shift, most pronounced in flowers, where *M. fructicola* increased richness (Chao1), diversity (Shannon), and dominance (Simpson). In wood samples, increased dominance suggested pathogen-associated ecological filtering. Network analysis demonstrated that *M. fruticola* disrupts fungal connectivity, leading to fragmentation of microbial interactions, reduced network complexity, and increased modularity – indicative of weakened ecological cohesion. Shifts in fungal primary lifestyles further suggested that *M. fructicola* accelerates tissue decomposition and induces an imbalance in functional guilds, potentially facilitating secondary infections. Taxonomic restructuring was marked by the decline of dominant genera and the emergence of stress-adapted or pathogen-associated taxa. The isolation of *Epicoccum nigrum*, a known biocontrol agent, highlights its potential as a nature-based solution for disease management. Overall, these findings identify *M. fructicola* as a driver of

fungal dysbiosis in *P. persica*, with cascading effects on microbial function, network resilience, and plant health. Understanding these pathogen-induced shifts is essential to inform sustainable microbiome-based approaches to disease management.

Keywords: Mycobiota, Dysbiosis, *Monilina fructicola, Prunus persica*; Fungal Community Structure, Disease Ecology

Introduction

The peach tree (*Prunus persica* (L.) Batsch) is a deciduous tree or shrub of the *Rosaceae* family, widely cultivated worldwide (Zheng et al., 2014). Archaeological evidence suggests that *Prunus* species were first domesticated in northwestern China (Li, 1978), which remains the global centre of peach production. In 2023, China produced approximately 17.50 million tonnes of peaches, accounting for 61.12% of the global production, followed by Spain (1.31 million tonnes), Turkey (1.07 million tonnes), and Italy (1.03 million tonnes). Other producing countries include Portugal, where the Cova da Beira region is the main producing area for peaches and nectarines (FAOSTAT, 2023). According to Portuguese statistics, peach and nectarine production reached 34,776 tonnes, of which 18,706 tonnes were produced in central Portugal (INE, 2020).

Beyond their economic value, peaches are nutritionally valuable stone fruits, rich in vitamins, flavonols, sugars, catechins and dietary fibre, contributing to human health benefits (Liao et al., 2019; Pakbin et al., 2014). In addition to fresh consumption, peaches are processed into canned and dried fruit, juices, and snacks. Peach trees are also highly valued as ornamental plants due to their striking white, pink, or red flowers that bloom in spring (Luo et al., 2022). However, despite their agricultural and aesthetic importance, peach production faces major phytosanitary challenges. Pre-harvest and post-harvest diseases can significantly reduce fruit yield and quality and, in severe cases, compromise tree longevity (Sisquella et al., 2014).

Among these threats, fungal and bacterial diseases pose significant risks to commercial peach cultivation. Several fungal pathogens infect different plant tissues, including leaves (*Taphrina deformans* (Berk.) Tul. - peach leaf curl disease; *Stigmina carpophila* (Lév.) M.B. Ellis - shot-hole disease; *Chondrostereum purpureum* (Pers.) Pouzar

- silver disease), trunk and branches (*Diaporthe amygdali* (Delacr.) Udayanga, Crous & K.D. Hyde - canker and dieback diseases, *Cytospora leucostoma* (Pers.) Sacc. - leucostoma canker), and fruits (*Podosphaera pannosa* (Wallr.) De Bary - powdery mildew), *Monilinia* sp. - brown rot) (Luz, 2014). Due to their impact on plant health, some of these pathogens are classified as quarantine pests by the European and Mediterranean Plant Protection Organization (EPPO). The A2 quarantine list includes *Pseudomonas syringae* pv. *persicae*, *Xanthomonas arboricola* pv. *pruni* (both bacteria), *Monilinia fructicola* (G. Winter) Honey (fungus), and Plum pox virus, as they are present in certain regions of the EPPO area but still pose a significant phytosanitary risk, requiring strict regulatory measures to prevent their further spread (EPPO, 2019).

In Portugal, Plum pox virus was first detected on the mainland in 1984 and later identified in the Azorean islands of Terceira and Graciosa (EPPO, 2020). The first confirmed detection of *M. fructicola* in Portugal occurred in the Cova da Beira region (Baltazar et al., 2023), a major peach and nectarine production area in Portugal. *Monilinia* spp., a major causal agent of brown rot in stone fruits, represents a significant threat to production, particularly in humid climates where pre- and post-harvest losses can reach up to 80% (Larena et al., 2005). Mummified fruits attached to trees serve as primary inoculum sources, enabling the pathogen to infect flowers and subsequently spread to developing fruit (Casals et al., 2022). The pathogen was identified following the appearance of unusual symptoms in localized orchards, including necrosis and abortion of flowers, canker formation with gum exudation on branches, and severe tree decline, sometimes leading to partial or total plant death. *M. fructicola* primarily infects flowers and woody tissues, causing blossom blight and twig dieback, making these plant structures particularly susceptible to its effects (Martini & Mari, 2014).

Plant-associated microbial communities inhabit various compartments, including the phyllosphere, rhizosphere, and endosphere, where they play fundamental roles in plant health by regulating nutrient uptake, stress tolerance, and pathogen resistance (Vorholt, 2012). These microbial consortia do not function in isolation but rather form a complex and dynamic network with the host, collectively referred to as the holobiont. This concept recognizes that plant health and adaptability are shaped by its interactions with the associated microbiota,

emphasizing the functional integration of microbes in plant physiology and resilience (Vandenkoornhuyse et al., 2015).

The plant microbiota is shaped by both vertical transmission (via seeds or clonal propagation) and horizontal acquisition from the surrounding environment, with plants actively selecting microbial partners in response to biotic and abiotic factors (Bodenhausen et al., 2014; Chen et al., 2020). The assembly and stability of these communities depend on a combination of stochastic and deterministic processes, which regulate microbial interactions and define host-microbiome relationships (Vandenkoornhuyse et al., 2015). However, this delicate balance can be disrupted by environmental stressors, pathogen infections, or host dysfunction, leading to a state of microbial imbalance known as dysbiosis (Arnault et al., 2023).

Advances in next-generation sequencing (NGS) technologies have significantly expanded our understanding of microbial diversity in agriculture and plant health. Traditionally, microbiome studies relied on culturable methods, which capture only a small fraction of microbial diversity. High-throughput sequencing now enables the massive profiling of environmental samples, providing insights into microbial community composition, structure, and function (Dubey et al., 2022). This approach has revealed previously undetected microbial taxa, tracked community dynamics, and explored microbial interactions in unprecedented detail.

Dysbiosis is characterized by an imbalance in microbial communities, often associated with a decline in the host's ability to regulate its microbiota. This loss of control can result in functional impairments, including weakened pathogen suppression, altered nutrient dynamics, and reduced stress resilience (Arnault et al., 2023). While dysbiosis is frequently associated with decreased microbial diversity, some studies suggest that it can also be linked to an increase in diversity due to the chaotic colonization of new niches by opportunistic microorganisms (Gibbons et al., 2016). The Anna Karenina Principle (AKP) predicts that disease-associated microbiomes exhibit greater variability than healthy ones due to the disruption of host control over microbial community assembly (Ma, 2020; Zaneveld et al., 2017). This model, widely applied to animal microbiomes, including humans, corals, and other host-associated microbial systems (Arnault et al., 2023; Ma, 2020), has recently been adapted to plant systems (Ahmed et al., 2019). An alternative model, ANTI-AKP, suggests

that under stress conditions, plants may actively recruit beneficial microbes to restore microbiome balance through deterministic selection. This hypothesis is based on the idea that plants, rather than passively losing microbiome stability, may selectively enrich specific microbial consortia to counteract pathogens and improve stress resilience (Arnault et al., 2023). This "cry for help" strategy suggests that microbial shifts in response to disease are not purely stochastic but may follow predictable patterns of beneficial microbial recruitment (Vorholt, 2012).

Pathogens play a crucial role in disrupting microbial networks and reshaping plant-associated communities (Vannier et al., 2015). In peach trees, fungal infections—particularly those caused by quarantine pathogens such as *M. fructicola* - are likely to drive significant shifts in fungal community composition and structure. Given that *M. fructicola* primarily infects flowers and woody tissues, it provides an ideal model for studying pathogen-induced dysbiosis in perennial hosts.

The recent detection of *M. fructicola* in Portugal presents a unique opportunity to investigate its impact on fungal communities in peach trees under field conditions. During the spring seasons of 2021 and 2022, field surveys were conducted in orchards exhibiting cankers, gummosis, flower abortion, mummified fruits, and tree decline. *M. fructicola* was identified in multiple orchards, allowing for comparative sampling of infected and non-infected plants.

This study aimed to determine how *M. fructicola* influences fungal community composition, diversity, and function by analyzing wood and flower samples. By comparing the mycobiota of pathogen-infected and pathogen-free samples, we assess whether *M. fructicola* acts as a driver of dysbiosis. To strengthen our findings, we also isolated and identified fungal pathogens from all samples.

Materials and Methods

Study Area, Sampling Procedures and Detection of *Monilinia fructicola*

The sampling was conducted in the Cova da Beira region, in the municipalities of Fundão, Covilhã, and Belmonte within the Castelo Branco district, Portugal. A total of 14 orchards of peach were sampled during the spring of 2021 and 2022. The plant material collected for this study included flowers and wood. A total of 32 composite samples were collected from

symptomatic branches (26 samples) and flowers (6 samples), including necrosis, flower abortion, and cankers with gummosis exudation. Two samples were later removed after being identified as belonging to *Prunus avium*. Each composite sample consisted of a pool of tissues (flowers and/or branches) (Supplementary Figure S1) collected from at least three symptomatic plants within the same orchard, ensuring a representative capture of observed symptoms. Samples were placed in sterile bags, kept on ice, and transported to the laboratory, where they were processed the following day. Samples were then placed in a Bioreba bag containing 5 mL phosphate-buffered saline (PBS) per gram of sample and macerated using a homogenizer (Homex 7, Bioreba, Reinach, Switzerland). For maceration, approximately 15–20 g of flowers or 45–50 g of woody branches were used per sample. Total DNA was extracted using the Dneasy Plant Kit (Qiagen, Venlo, The Netherlands) according to the manufacturer's instructions and stored at -20°C. A duplex real-time PCR assay, developed by Van Brouwershaven et al., 2010 and included in EPPO standards (EPPO, 2020), was used to detect *Monilinia* sp. in some plant samples (Supplementary Table S1). This protocol distinguishes between *M. fructicola, M. fructigena* and *M. laxa*. As positive controls, cultures of *M. fructicola* CECT 21105, *M. fructigena* CECT 21206, and *M. laxa* CECT 21100 were obtained from the Spanish Type Culture Collection, which is housed at the University of Valencia. To further characterize the fungal communities present in the collected samples, high-throughput sequencing of the Internal Transcribed Spacer (ITS) region was performed.

Sample Preparation, Illumina Sequencing and Data Analysis

For library construction and sequencing, the total DNA previously extracted from the 32 samples was processed by Novogene (Germany) (Supplementary Table S1). DNA integrity, purity, fragment size, and concentration were initially assessed via agarose gel electrophoresis as part of the quality control process. Novogene then constructed Illumina ITS (Internal Transcribed Spacer) gene amplicon libraries, adding unique indexes to enable sequence assignment to each original sample. The quality and quantity of these libraries were subsequently determined using qPCR. Based on this quantification and the required data output, the libraries were pooled and sequenced on an Illumina NovaSeq paired-end platform (250 bp), performed by Novogene. For amplicon generation, PCR amplification of the ITS2 target region was performed using the primers 5′-GCATCGATGAAGAACGCAGC-3′

(ITS3) and 5′-TCCTCCGCTTATTGATATGC-3′ (ITS4), which were linked to barcodes. PCR products of the correct size were selected via 2% agarose gel electrophoresis. Equal amounts of PCR products from each sample were pooled, end-repaired, A-tailed, and ligated with Illumina adapters. The final libraries were sequenced as 250 bp paired-end reads. Following sequencing, the resulting set of Illumina paired-end demultiplexed fastq files, which included barcodes, were processed and assigned to samples using the QIIME2 platform (version 2024.2) (Bolyen et al., 2019) with the ITSxpress software (version 1.8.1)(Rivers et al., 2018) and DADA2 software (Callahan et al., 2016) plug-ins. Briefly, raw sequences were first imported into QIIME2. To specifically trim the ITS2 region, merge sequences, and remove the non-fungal sequences, the ITSxpress plugin was applied with the parameters (--p-region ITS2, --p-taxa F and --p-cluster-id 0.95). Raw paired-end reads were then denoised and assembled using the DADA2 plug-in, producing non-chimeric Amplicon Sequence Variant (ASV) Tables that described the composition of the fungal communities. ASVs were taxonomically assigned using the QIIME2 q2-feature-classifier plugin (Bokulich et al., 2018) against the UNITE reference database (Abarenkov et al., 2024). A pre-trained Naive Bayes taxonomic classifier was used based on the UNITE QIIME release for Fungi (version 04.04.2024, v10.0), with reference sequences clustered at 99% sequence similarity. A final taxonomy table was constructed at the end of the annotation step, and a rooted phylogenetic tree was generated using the QIIME2 Mafft program, followed by the FastTree algorithm. Finally, the ASV abundance, taxonomy Tables, and phylogenetic tree were exported along with representative sequences for subsequent statistical analysis in R.

Diversity Indexes and Statistical Analysis

All statistical analyses and visualizations were performed in R (version 4.4.1) (Team, 2024). Sequences were filtered to remove all unidentified phyla and ASVs with fewer than two reads and then rarefied to an equal depth. The calculation and rarefaction were conducted using the vegan package in R (version 2.6-8) (Oksanen et al., 2024).

Alpha diversity was calculated to assess the fungal richness and evenness within each wood and flower sample (Thukral, 2017). The Phyloseq package in R (version 1.46.0) (McMurdie & Holmes, 2013) was used to compute the Chao1, Shannon, and Simpson indices. To compare diversity indices among sub-groups, we performed T-tests for normally distributed

data and the non-parametric Mann-Whitney U test for data that did not meet normality assumptions.

To evaluate the Beta diversity of the wood and flowers mycobiome, the ASV absolute frequencies were first transformed to proportions and then subjected to a Principal Coordinates Analysis (PCoA) using the Unifraq dissimilarity distance. A PERMANOVA test was conducted to assess the statistical significance of the observed patterns. The adonis2 function was used with the Unifraq dissimilarity metric and 10,000 permutations to test for statistical significance. The analysis evaluated the influence of sample tissues and *M. fructicola* infection on the fungal community composition.

To further analyze the mycobiome data from the two types of samples, ASV absolute counts were transformed into relative abundances and aggregated at phylum, family and genus levels with the microbiome package in R (version 1.23.1) (Lahti & Shetty, 2017). This aggregation was performed with a detection threshold of 0.02 for the family level and 0.05 for the genus levels, meaning that taxa with relative abundances below 2% and 5%, respectively, were grouped into a single category called "Others". To visualize overlapping and unique fungal taxa across the different factors, a Venn diagram was created at the genus level using the ggvenn package in R (version 0.1.10) (Linlin, 2023). The FungalTrait database (Põlme et al., 2020; Tanunchai et al., 2023) was used to assign primary lifestyles to the genus taxonomic category. Heat maps of genus-level abundance and primary lifestyles were generated using the ggplot2 package in R (version 3.5.1) (Wickham, 2016). Differential abundance analysis of fungal genera and primary lifestyles between samples with and without *M. fructicola* was performed using the DESeq2 R package (v1.46.0) (Love et al., 2014) with default parameters, unless stated otherwise. For genus-level analysis of wood samples, a prevalence filter was applied to retain only genera present in at least 15% of the samples. Additionally, for both wood and flower datasets, a minimum abundance threshold of 0.1% of total reads was used to exclude very low-abundance taxa, to reduce background noise and improve the robustness of the statistical analysis. No prevalence or abundance filters were applied to the primary lifestyle analysis.

Co-occurrence networks

Co-occurrence networks were deployed to evaluate fungal interactions in wood samples, as the number of flower samples was insufficient for a reliable analysis. For the wood sample,

co-occurrence networks were constructed separately at the genus and at the ASV taxonomic levels. First, ASVs were aggregated at the genus level, and the dataset was then subset based on *M. fructicola* detection status (detected vs. not detected). Correlations were calculated using the Spearman method, with a correlation threshold of > 0.8 and p-values < 0.01, using the Hmisc package in R (version 5.2.1) (Harrell Jr, 2024). Networks were then constructed using the igraph package (version 2.1.2) (Csárdi & Nepusz, 2006). Network properties were calculated using the igraph package. The modularity score was determined using the Fast Greedy modularity optimization algorithm. To identify influential taxa within these networks, hub scores were calculated for each node using the hub score function from the igraph R package. Nodes with higher hub scores are considered to be more central within the network, potentially playing more significant roles in community structure and dynamics (Layeghifard et al., 2018). For the genus-level network, genera were ranked by their hub scores, and those with the highest scores were designated as "key genera". Network visualizations were generated using the ggraph package (version 2.2.1) (Pedersen, 2024). Additional co-occurrence networks were constructed at the ASV level following the same procedure. Similarly, for the secondary network constructed at the ASV level, ASVs were ranked by their hub scores, and those with the highest scores were designated as "key ASVs". This finer-scale ASV-level analysis, focusing on these hub ASVs, was performed to gain a more detailed understanding of potential interactions that might be obscured by genus-level aggregation, which is particularly relevant in phytopathological studies where subtle genetic variations can be important. These analyses provide insights into the structure and key features of fungal networks under different *M. fructicola* detection statuses in wood samples.

Fungal isolation, cultivation and molecular identification

For fungal cultivation, only branch segments were used, as flowers were highly vulnerable to the sterilization method, which caused tissue damage, rendering them unsuitable for this approach. Symptomatic woody branch segments from 20 composite samples collected across 11 orchards were used for fungal isolation. The samples were surface sterilized following the protocol described by (Eevers et al., 2015) and plated on potato dextrose agar (PDA) medium supplemented with streptomycin (0.5 g/L) to prevent bacterial growth, followed by incubation at 22 ºC in the dark for 7 days (Supplementary Figure S1). These samples

represent a subset of the original collection used for metabarcoding analysis (for details See Supplementary Table S1). For DNA extraction, pure fungal cultures from 58 isolates were processed after 7 days of mycelial growth using the REDExtract-N-Amp™ Plant PCR kit (Sigma Aldrich, St. Louis, MI, USA) following the manufacturer's instructions. The genomic DNA obtained was used for the amplification of the ITS-rDNA region by PCR, using the universal primer pair ITS1 (50-TCCGTAGGTGAACCTGCG-30) and ITS4 (50-TCCTCCGCTTATTGATATGC-30) (White et al., 1990). PCR reactions, with a final volume of 25 μL, consisted of 12.5 μL of NZYTaq Green Master Mix (NZYTech™, Portugal), 1 μL of each primer (10 mM), 8.5 μL of ultra-pure water and 1 μL of template DNA, were performed using a T100 Thermal Cycler (BIO-RAD), with the following conditions: initial denaturation at 94 °C for 5 min, followed by 34 cycles of denaturation at 94 °C for 1 min, annealing at 57 °C for 30 sec, and extension at 72 °C for 45 sec, with a final extension step at 72 °C for 10 min (White et al., 1990). The resulting amplified fragments were purified using the NZYGelpure Kit (NZYTech™, Lisbon, Portugal) and sequenced with the ITS4 (50-TCCTCCGCTTATTGATATGC-30) standard sequencing primer at STABVIDA, Caparica, Portugal. The obtained DNA sequences were processed using BIOEDIT 7.2, and a representative sequence of each species was deposited in the GenBank database. For molecular identification, these sequences were compared with sequences available in the National Center for Biotechnology Information (NCBI) using the Basic Local Alignment Search Tool BLAST (Altschul et al., 1990).

Results and discussion

Fungal Composition Shifts and Dysbiosis in *P. persica* Infected by *Monilinia fructicola*

While the concept of dysbiosis is well established in human microbiome research, its application in plant-associated fungal communities remains less defined, with no universally accepted metric or diagnostic threshold. In this study, we use the term dysbiosis in a conceptual sense, referring to pathogen-associated disruptions in community structure, diversity, and ecological balance. By comparing fungal communities between *Monilinia fructicola*-infected and non-infected *Prunus persica* tissues, we explore whether this quarantine pathogen acts as a driver of microbial imbalance consistent with dysbiosis.

To investigate whether this imbalance could result from pathogen-induced restructuring, the influence of *M. fructicola* on fungal community composition, diversity, and function was analyzed in wood and flower samples. To investigate its potential impact, a total of 32 samples were collected from multiple *Prunus persica* orchards, four of which tested positive for this quarantine fungus. By comparing the mycobiota of pathogen-infected and pathogen-free samples, we assessed whether *M. fructicola* acts as a driver of dysbiosis, providing a basis for determining the fungal composition in orchards where *M. fructicola* was detected (MF-D) and those where it was not detected (MF-ND). DNA was extracted, and fungal diversity was analyzed using ITS metabarcoding coupled with high-throughput sequencing (Supplementary Table S2). A total of 2,669,379 high-quality sequences were obtained, with an average of 66,735 sequences per sample for the fungal ITS2 gene. After the ASV assignment, an average of 998 fungal ASVs remained (Supplementary Table S3). To standardize sequencing depth across samples, data were rarefied to a minimum library size of 13,190 reads, after which all rarefaction curves reached saturation, confirming that the sequencing depth was sufficient to capture the microbial community diversity. Of the total of 32 samples sequenced. Two samples originating from *Prunus avium* were excluded from the analysis as previously described. Four samples with read counts below the rarefaction threshold were removed before rarefaction. This resulted in a final dataset of 26 samples for downstream analysis. This approach enabled a comparative analysis of fungal communities in trees infected and non-infected by *M. fructicola* to determine whether the pathogen alters mycobiota structure and contributes to dysbiosis.

In wood samples, MF-ND samples were dominated by *Ascomycota* (94.6%) with *Basidiomycota* accounting for only 5.1% of the community (Supplementary Figure S2). In contrast, MF-D wood samples exhibited a shift in relative abundance, with *Ascomycota* decreasing to 87.9% and *Basidiomycota* increasing to 11.5% (Supplementary Figure S1). A similar trend was observed in flowers, where MF-ND samples comprised 91.2% *Ascomycota* and 8.8% *Basidiomycota*, while MF-D flower samples exhibited a further decrease in *Ascomycota* (81.8%) and a corresponding increase in *Basidiomycota* (16.6%) (Supplementary Figure S1). These patterns suggest that the transition from MF-ND to MF-D status in both wood and floral tissues is associated with a decrease in the relative abundance of *Ascomycota* and enrichment of *Basidiomycota*; this trend is consistent with other studies

in tobacco (Zheng et al., 2022), and in strawberry (Zhang et al., 2023). The prevalent presence of *Ascomycota* and *Basidiomycota* phyla is consistent with previous studies that indicated plant mycobiota is predominantly composed of these groups (Hortová & Novotný, 2011; Sun & Guo, 2012; Müller et al., 2016). Additionally, *Ascomycota* fungi have been reported to exhibit greater species diversity due to their higher evolutionary rate and adaptability (H. Wang et al., 2010), which aligns with our results, where *Ascomycota* was the dominant phylum across all samples independently of the tissue type.

Notably, in wood samples, six fungal phyla were identified: *Aphelidiomycota*, *Ascomycota*, *Basidiomycota*, *Blastocladiomycota*, *Chytridiomycota*, and *Mortierellomycota*. However, the dominant phyla were *Ascomycota* and *Basidiomycota*, which collectively accounted for the vast majority of sequences (e.g., >95% of reads). The remaining four phyla (*Aphelidiomycota*, *Blastocladiomycota*, *Chytridiomycota*, and *Mortierellomycota*), while detected, were present at very low relative abundances, with the total reads assigned to each of these phyla being well below 1% of the community. Consequently, the individual ASVs belonging to these less common phyla were also found at relative abundances below the 1% threshold. In contrast, flower samples displayed lower fungal diversity at the phylum level, with only *Ascomycota* and *Basidiomycota* detected, both at high relative abundances (Supplementary Figure S2). These findings suggest a broader fungal diversity in wood compared to flowers, potentially linked to differences in microhabitat stability, substrate availability, and selective pressures between these tissues.

At the family level, fungal community composition also differed between MF-D and MF-ND groups in both wood and flower, highlighting shifts associated with the presence of *M. fructicola* (Figure 1). In wood samples (Figure 1a), the most abundant families for the MF-ND group were *Saccotheciaceae* (41.8%), *Sclerotiniaceae* (35.8%), and *Bulleribasidiaceae* (4%). In the MF-D group, *Saccotheciaceae* remained dominant (47.2%), but *Sclerotiniaceae* decreased to 11.1%, while *Bulleribasidiaceae* increased to 10%. In flower samples (Figure 2b), *Saccotheciaceae* was the predominant family in the MF-ND samples (87.5%), followed by *Bulleribasidiaceae* (8.2%) and *Diaporthaceae* (0.9%). Conversely, in MF-D samples, *Saccotheciaceae* declined to 72.9%, while *Bulleribasidiaceae* increased to 13.8% and *Taphrinaceae* emerged as a more abundant family (2.6%).

To further explore fungal community differences, the presence of fungal genera between orchards with and without *M. fructicola* was compared using Venn diagrams (Figure 2). Overall, shared genera account for 95.2% of the abundance in wood samples and 97.8% in flower samples. In detail, in wood samples (Figure 2a), 26 genera (27.2%) were shared, while 80 genera (62%) were unique to MF-ND and 23 genera (17%) were unique to MF-D, totalling 129 fungal genera. In flower samples (Figure 2b), 17 genera (38.6%) were shared, while 15 genera (25.4%) were unique to MF-ND and 27 genera (45.8%) were unique to MF-D, totalling 59 fungal genera. These results highlight distinct fungal genus distributions between infected and non-infected trees, reinforcing the hypothesis that *M. fructicola* influences fungal diversity and potentially drives dysbiosis.

The relative abundance of fungal genera exhibited shifts between MF-ND and MF-D groups (Figure 3, Supplementary Figure S3 and Supplementary Tables S4-S5), indicating that the presence of *M. fructicola* significantly influences fungal community structure. In wood samples (Figure 3a), several genera that were dominant in MF-ND samples showed a marked decline in MF-D samples, while others emerged or increased in abundance. The genus *Botrytis*, for example, showed a significant dramatic reduction (padj <0.001), decreasing from 13.9% in MF-ND samples to only 0.04% in MF-D samples. A similar trend was observed for *Diaporthe* and *Taphrina*, whose relative abundance declined from 1.3% to 0.02% and 1.5% to 0.02%, respectively, although only the first was significant (padj < 0.001 and padj = 0.31, respectively). Conversely, some fungal genera became more prevalent in MF-D samples, suggesting that *M. fructicola* may alter the fungal community composition by promoting the establishment of certain taxa. *Pycnopeziza*, which was completely absent in MF-ND samples, appeared in MF-D samples with a relative abundance of 7.6% (padj < 0.001). Similarly, *Cytospora* increased from 0.05% in MF-ND samples to 6.1% in MF-D samples, while *Vishniacozyma* more than doubled in abundance, rising from 4.3% to 10.0%, both of which were non-significant (padj = 0.34 and padj = 0.44, respectively).

In flower samples (Figure 3b), similar trends were observed, with several genera declining in MF-D samples while others became more abundant. *Alternaria* showed a slight non-significant reduction in relative abundance, decreasing from 0.46% in MF-ND samples to 0.33% in MF-D samples (padj = 0.11). A non-significant decline (padj = 0.21) was noted for *Podosphaera*, which declined from 0.17% to just 0.005%. *Diaporthe*, present at 0.88%

in MF-ND samples, was completely absent in MF-D samples. On the other hand, certain fungal genera increased in MF-D samples, suggesting a potential restructuring of the fungal community associated with the presence of *M. fructicola*. *Taphrina*, for example, exhibited a significant increase (padj = 0.0013), rising from 0.01% in MF-ND samples to 2.6% in MF-D samples. *Vishniacozyma* showed a non-significant increase (padj = 0.90), rising from 8.2% to 13.8%.

These results suggest that the presence of *M. fructicola* is associated with both a decline in certain fungal taxa and the proliferation of others, leading to a pathogen-driven restructuring of fungal communities. The emergence of *Pycnopeziza* and *Cytospora* in MF-D samples, along with the increased abundance of *Vishniacozyma*, indicates that *M. fructicola* may create conditions favourable for the establishment of specific fungal groups while simultaneously suppressing others. Among these taxa, *Vishniacozyma,* a genus of yeast belonging to the *Bulleribasidiaceae* family, stands out due to its reported antagonistic properties, enzymatic activity, and ability to form biofilms (Nian et al., 2023). Although its increase in abundance was not statistically significant, the identification of two key ASVs belonging to this genus in the co-occurrence network analysis (described in detail in the following sections) supports the hypothesis of a potential ecological role within the community. In fact, given its known biocontrol potential, it is plausible that *M. fructicola* indirectly facilitates the proliferation of *Vishniacozyma* as part of a microbial network dynamic that suppresses other fungal pathogens. This could represent an opportunistic strategy by *M. fructicola*, leveraging the presence of *Vishniacozyma* to reduce competition from other fungal taxa and reinforce its ecological dominance. Interestingly, the relative abundance of the genus *Taphrina* decreased in wood samples infected with *M. fructicola* but increased in infected flower samples. *Taphrina* includes plant-pathogenic fungi known to infect young, actively growing tissues, often causing distortions such as leaf curls and witches' brooms by interfering with host cell division and expansion (Thangaraj et al., 2025). One possible explanation for this contrasting pattern is the differing ecological niches and tissue types colonized by *Taphrina* and *M. fructicola*. In woody tissues, *M. fructicola* may outcompete or inhibit *Taphrina* through resource competition or antagonistic interactions. Conversely, in floral tissues, where both fungi may exploit softer, nutrient-rich environments, *Taphrina* could benefit from the disruption of host defenses or tissue damage caused by *M.*

fructicola, allowing it to proliferate. This pattern suggests a context-dependent interaction that warrants further investigation into the functional dynamics between these two pathogens.

The observed genus-level shifts further support the hypothesis that *M. fructicola* contributes to dysbiosis, particularly in flowers and wood, where alterations in microbial composition may influence plant health and disease progression. These findings highlight the need for further investigation into the functional interactions between *M. fructicola* and other fungal community members, particularly potential synergies or competitive exclusions mediated by yeast species such as *Vishniacozyma*.

Monilinia fructicola-Induced Shifts in Fungal Diversity and Community Structure

Microbial diversity plays a fundamental role in shaping ecological dynamics across different environments. In this study, we assessed fungal diversity in the wood and flowers of *Prunus persica* to determine whether the presence of the quarantine pathogen *M. fructicola* disrupts the natural mycobiota, potentially leading to dysbiosis. It is known that the microbial communities of flowers and other plant compartments, such as wood, can vary considerably (Aleklett et al., 2014). For subsequent analysis, two sub-groups were created by subsetting the initial sample data: wood (N = 20) and flowers (N = 6). To ensure statistical robustness, normality tests and variance homogeneity tests were performed to compare mycobiota diversity between tissue types (wood and flowers) (Supplementary Table S6).

To evaluate these changes, we analyzed alpha diversity indices, including Chao1 (species richness), Shannon (richness and evenness), and Simpson (D, dominance and evenness) (Supplementary Figure S3 and Supplementary Table S7). In wood samples, no significant differences were observed between MF-D and MF-ND groups for the Chao1 and Shannon indices, indicating stable overall richness and diversity in infected trees (Supplementary Table S7). However, the Simpson index showed a significant difference (t-test, $p = 0.04946$), suggesting that *M. fruticola* increases species dominance, potentially through competition of less adapted taxa (Supplementary Table S7). In contrast, flower samples exhibited significant shifts in fungal diversity associated with the presence of *M. fructicola* (Supplementary Figure S3b). The Chao1 index (t-test, $p = 0.00908$) revealed higher richness in the MF-D group, suggesting that pathogen presence correlates with an expansion of fungal diversity. The Shannon index (t-test, $p = 0.03121$) confirmed greater overall

diversity in this group, while the Simpson index (t-test, $p = 0.04097$) demonstrated increased species dominance in infected flowers (Supplementary Table S7). These patterns suggest that infection by *M. fructicola* in flowers may promote microbial competition and restructuring of the mycobiota, potentially driven by host stress responses or pathogen-induced ecological filtering.

Beta-diversity analysis further supports these findings, highlighting a stronger pathogen-driven shift in fungal community composition in flowers compared to wood. Using UniFrac distances and Principal Coordinate Analysis (PCoA), we observed that in wood samples (Figure 4a), MF-D and MF-ND groups did not form distinct clusters, although samples with *M. fructicola* detected tended to group. This suggests that while the pathogen presence influences community composition, wood-associated fungal communities may be more resilient to structural shifts. PERMANOVA analysis supported this observation, revealing a significant effect of infection status on fungal community structure ($R^2 = 0.098$, $p = 0.009$), with the presence of *M. fructicola* explaining approximately 9.8% of the total variation in the fungal community. In flower samples (Figure 4b), a clear separation along the first axis was observed between MF-D and MF-ND groups, indicating a stronger pathogen-driven shift in community composition compared to wood. However, the small sample size likely contributed to the lack of statistical significance in the PERMANOVA analysis ($R^2 = 0.364$, $p = 0.1$). The proportion of variance explained by the first two axes is 19.9% and 13.5% for wood samples, and 38.1% and 23.6% for flower samples, respectively, reinforcing that *M. fructicola* exerts a stronger effect on fungal communities in flowers than in wood.

Overall, these results indicate that *M. fructicola* differentially impacts fungal communities in *P. persica* tissues, with infection leading to microbial restructuring in flowers but a more limited effect in wood. Applying the Anti-AKP principle (Arnault et al., 2023), our findings suggest that *M. fructicola* induces deterministic shifts in fungal communities, particularly in flowers, where increased richness (Chao1), diversity (Shannon), and species dominance (Simpson) indicate an organized microbial restructuring. Although we did not assess plant immune responses directly, such structured community shifts may be consistent with the hypothesis that plant stress responses - potentially including pattern-triggered immunity (PTI) and effector-triggered immunity (ETI) - can contribute to the selective

recruitment of beneficial microbes (Arnault et al., 2023; Vorholt, 2012). In this view, microbial selection is not based on active discrimination between beneficial and harmful taxa, but rather on the ecological filtering effects of host responses. In contrast, wood samples exhibit minimal changes in richness or diversity, though the increased species dominance (Simpson index) suggests that *M. fructicola* may be driving ecological filtering, favouring competitive taxa over others. This effect, while still deterministic, appears less pronounced in wood, possibly due to lower microbial turnover rates or a more stable microhabitat.

These findings align with other studies showing that pathogen presence can reshape plant-associated microbiomes. For instance, Bez et al. (2021) demonstrated that the rice foot rot pathogen *Dickeya zeae* significantly altered the in-field plant microbiome, leading to increased biodiversity in symptomatic plants. Similarly, Closek et al. (2014) found that bacterial communities associated with tropical coral hosts exhibited greater diversity in diseased samples, highlighting a broader trend in pathogen-driven microbiome shifts. However, it remains unclear whether increased microbial diversity is a cause or a consequence of microbiome-associated diseases (Ma et al., 2019). While some studies suggest that higher diversity characterizes healthier microbiomes, others report that dysbiosis can also be associated with increased alpha diversity, as seen in cases of human microbiota imbalance (Lozupone et al., 2012; Lamelas et al., 2020). This apparent contradiction underscores the need to consider not only diversity metrics but also microbial community composition and ecological interactions when assessing pathogen-induced dysbiosis. Moreover, the plant's fitness is likely influenced by the organized biodiversity of its microbiome, which plays a crucial role in enabling rapid adaptation and plasticity to environmental changes (Vandenkoornhuyse et al., 2015).

Although we did not apply a formal metric for dysbiosis - given the absence of such tools in plant-associated fungal systems - the convergence of evidence observed in our study supports the hypothesis that *M. fructicola* induces microbial dysbiosis in *P. persica*. Alterations in alpha and beta diversity, loss of dominant taxa, reduced genera overlap, and the emergence of new genera and functional shifts collectively indicate an infection-associated reconfiguration of the fungal community. These effects were particularly marked in floral tissues, reinforcing the notion that pathogen pressure may destabilize microbial networks and drive ecologically relevant changes in the mycobiota.

Functional Disruptions and Trophic Shifts Induced by *M. fructicola*

Fungal trophic strategies play a crucial role in maintaining microbial balance in plant-associated communities. To assess how *M. fructicola* influences fungal functional guilds, we analyzed the relative abundance of different primary lifestyles in wood and flower samples from *P. persica* trees with and without pathogen detection (Figure 5 and Supplementary Tables S8 -S9). In wood samples (Figure 5a), the most dominant primary lifestyle in MF-ND samples was "Plant Pathogen" (18.3%), but this category significantly decreased to 6.9% in MF-D samples (padj < 0.001), suggesting that the presence of *M. fructicola* may suppress other pathogenic fungi. A similar pattern was observed for "Mycoparasites," which declined from 0.26% in MF-ND to 0.10% in MF-D samples (p = 0.20), possibly reflecting competitive exclusion effects. In contrast, several saprotrophic lifestyles increased in the presence of the pathogen. Notably, "Litter Saprotrophs" rose markedly and nearly significantly in MF-D samples (8.4%) compared to MF-ND (1.0%) (padj = 0.06), while "Soil Saprotrophs" more than doubled (10.1% in MF-D vs. 4.5% in MF-ND) (although not significantly, with padj = 0.73), indicating a potential shift toward decomposer fungi, maybe as a result of host tissue degradation caused by infection. Minor categories such as "Wood Saprotrophs" and "Unspecified Saprotrophs" showed slight variation and remained below 0.2% in both sample groups. The proportion of unclassified or unassigned taxa ("NA") was slightly lower in MF-D samples (27.3%) than in MF-ND (33.6%) (padj = 0.15), which could indicate the presence of well-characterized taxa that may play a role in pathogen-associated dysbiosis.

In flower samples (Figure 5b), "Soil Saprotrophs" were the dominant lifestyle category in both groups, increasing from 8.2% in MF-ND samples to 13.8% in MF-D samples. The relative abundance of "Plant Pathogens" also doubled in infected samples (3.7% in MF-D vs. 1.7% in MF-ND), in contrast with the pattern observed in wood, where pathogenic taxa decreased. As described in the previous section, the genus *Taphrina*, which includes known plant pathogens, also increased in infected flower samples, reinforcing the idea that *M. fructicola* may facilitate the establishment of other pathogenic fungi in floral tissues. "Litter Saprotrophs" also increased slightly in infected flowers (0.8% in MF-D vs. 0.4% in MF-ND), while "Unspecified Saprotrophs" followed a similar trend (0.7% in MF-D vs. 0.3% in MF-ND), indicating a general enrichment of saprotrophic lifestyles. The

proportion of "Mycoparasites" slightly decreased in MF-D samples (0.09% vs. 0.13%), remaining a minor component in both groups. Contrary to wood samples, unassigned taxa ("NA") increased in MF-D samples (8.0% vs. 1.7%), which could indicate taxonomic shifts that remain undetected using current classification databases. Of note, all observed changes were statistically non-significant (adjusted *p*-values ranging from 0.36 to 0.91), possibly reflecting the limited sample size for flowers (3 MF-ND and 3 MF-D samples)

The observed shifts in primary lifestyles suggest that *M. fructicola* infection disrupts the balance between pathogenic and saprotrophic lifestyles, fungi in *P. persica*. In wood, the decline in pathogens and increase in saprotroph groups suggests that the pathogen *M. fructicola* may accelerate tissue decay, potentially altering the fungal succession dynamics in infected branches. In flowers, however, the increase in both saprotrophic and pathogenic taxa suggests that *M. fructicola* may facilitate the colonization of other opportunistic fungi, potentially exacerbating disease progression. These findings align with previous studies demonstrating that pathogen presence can reshape microbial communities through resource competition, niche displacement, and immune-mediated selection (Vannier et al., 2015). The increased abundance of saprotrophs in infected tissues suggests that *M. fructicola* may weaken host defences, allowing decomposer fungi to thrive.

Fungal Network Disruption Under *M. fructicola* Infection

Network analysis provides valuable insights into microbial interactions and community dynamics, particularly under biotic stress conditions. Given the limited number of flower samples (N < 4), co-occurrence network inference was conducted exclusively on wood samples to assess the impact of *M. fructicola* on fungal community connectivity and structure. The results indicate that the pathogen significantly alters fungal interactions, leading to substantial network disruptions between MF-ND and MF-D samples (Figure 6).

The fungal network in MF-ND samples (N = 9) (Figure 6a) was considerably larger, comprising 106 nodes and 705 edges, whereas the MF-D network (N = 11) (Figure 6b) was drastically reduced to 49 nodes and 32 edges. This reduction in network size and connectivity suggests that *M. fructicola* infection leads to a marked loss of interaction complexity in the fungal community of infected trees. Average node connectivity, a key indicator of how well-connected taxa are within the network, was higher in the MF-ND network (13.30) compared

to MF-D samples (1.31), indicating that fungi in pathogen-free wood form a more cohesive and interactive community. The average path length, representing the average number of steps required to connect any two nodes, was slightly higher in MF-ND samples than in MF-D samples, reinforcing the hypothesis that pathogen presence leads to a fragmentation of fungal interactions. Similarly, the network diameter, representing the longest shortest path between two nodes, was 5 in the MF-ND network but only 1 in the MF-D network, suggesting that fungal taxa in pathogen-infected trees exist in a more isolated and dispersed manner.

Interestingly, while overall connectivity declined, the clustering coefficient, which measures the tendency of nodes to form tightly connected groups, was slightly higher in the MF-D samples (1.00) compared to MF-ND samples (0.95). This suggests that, despite the drastic reduction in interactions, the remaining fungal taxa formed more compact and segregated communities. Moreover, the modularity score, which reflects the degree of network compartmentalization, was higher in the MF-D samples (0.81) than in MF-ND samples (0.47), further supporting the hypothesis that *M. fructicola* infection leads to a more fragmented and compartmentalized fungal network.

The resulting network, constructed at the genus level, allowed for the identification of key genera, defined here as those genera exhibiting the highest hub scores (see Methods for details), indicating their pivotal role in structuring the fungal community in MF-ND and MF-D samples at this taxonomic resolution. In pathogen-free samples, the most highly connected and influential taxa included *Pseudodidymosphaeria*, *Periconia*, *Chaetosphaeronema*, *Paraphoma*, and *Phaeosphaeria*. These genera are likely involved in wood degradation, nutrient cycling, and pathogen suppression, contributing to the stability of the fungal network. In contrast, MF-D samples exhibited a distinct fungal composition, with the dominance of *Rachicladosporium*, *Dothidotthia*, *Botrytis*, *Schroeteria*, and *Buckleyzyma*, suggesting that *M. fructicola* induces a shift in community composition, favouring fungal taxa that are adapted to stress or altered microenvironments. To further explore the fungal community structure with higher resolution, an additional co-occurrence network was constructed at the Amplicon Sequence Variant (ASV) level. From this ASV-level network, key ASVs were identified based on their hub scores (see Methods), representing ASVs deemed most central within this more detailed community framework. Examination of the key ASVs in the networks further revealed distinct taxonomic signatures

between the MF-ND and MF-D samples. In the MF-ND samples, ASVs were predominantly assigned to *Fusicolla* (2 ASVs), *Schizothecium*, and an unclassified *Agaricomycetes* and *Lophiostomataceae* genera, whereas in the MF-D samples, ASVs were largely assigned to *Phoma*, *Vishniacozyma* (2 ASVs), and *Dothidotthia* (2 ASVs).

In wood samples, the fungal community exhibited relatively stable ASV numbers, with *Vishniacozyma* showing nine ASVs in MF-ND samples and ten in MF-D samples, while both *Cytospora* and *Botrytis* consistently displayed one ASV under each condition. This pattern aligns with the increase in community evenness indexes observed in MF-D samples, despite the absence of a corresponding rise in richness. Conversely, flower tissues followed a different trend, displaying both an increase in richness and shifts in dominance patterns. For example, the number of ASVs assigned to *Vishniacozyma*, a key player in the fungal community of MF-D flowers, increased from four in MF-ND samples to ten in MF-D samples. Additionally, the *Taphrina* genera increase from one to three ASVs in MF-D samples, contributing to a potential restructuring of the fungal community toward a more diverse but dominant assemblage in infected floral tissues. These findings provide further support for the hypothesis that *M. fructicola* creates conditions that favour *Vishniacozyma*, potentially facilitating its establishment and activity within the fungal community. The observed increase in *Vishniacozyma* ASVs in infected flowers and its presence among the key taxa in MF-D networks suggest that this yeast may play a role in modulating community structure in response to *M. fructicola* infection. Given its known biocontrol properties, it is plausible that *Vishniacozyma* contributes to suppressing other fungal taxa, potentially benefiting *M. fructicola* by reducing competition from other pathogenic fungi.

The marked differences in the fungal community between flowers and wood tissues under *M. fruticola* infection may be linked to differences in tissue stability, resource availability, and microbial succession. Flowers, being transient and nutrient-rich, likely support a more dynamic fungal community that responds rapidly to infection, whereas wood tissues provide a more stable environment, favouring the persistence of mature microbial assemblages. These findings suggest that *M. fructicola* infection not only reduces fungal network connectivity and complexity but also drives taxonomic and structural shifts in fungal communities, with different responses in woody and floral tissues. This highlights the

pathogen's potential role as a driver of fungal community fragmentation and reorganization in *P. persica*.

Isolation and Molecular Identification of Pathogenic Fungal Species in *P. persica* orchards

The isolation and molecular characterization of fungal species complemented the high throughput sequencing approaches, providing a deeper understanding of fungal diversity, pathogenic potential and ecological role. Culturing fungal strains enables future studies on pathogen virulence, host interactions, and the development of biological control strategies leveraging naturally occurring antagonists. In this study, fungal diversity was assessed through the isolation and molecular identification of putative pathogenic fungal species using ITS rRNA gene fragment analysis.

A total of 58 fungal isolates, representing 19 different species, were successfully obtained from 11 orchards (Supplementary Table S10). All samples used for fungal isolation were collected from trees showing visible disease symptoms, including flower necrosis, abortion, gummosis, cankers on branches, and, in some cases, severe decline. Comparative sequence analysis confirmed the presence of several pathogenic species known to affect stone fruit trees. Canker diseases are primarily associated with the presence of *Diaporthe amygdali*, *Diaporthe ambigua*, *Cytospora leucostoma*, and *Botryosphaeria dothidea*, which predominantly affect woody tissues. These fungi are well-known for causing significant damage to fruit trees, particularly in stress-prone environments. *D. amygdali* is linked to dieback, cankers, leaf spots, blights, decay, and wilt (Thompson et al., 2011; Zhou et al., 2024). *Cytospora* species, responsible for cankers and tree decline in stone fruits, have been identified on 20 host species across nine genera within the *Rosaceae*, including *Malus*, *Prunus* and *Pyrus* (Fan et al., 2020). More specifically, *C. leucostoma* is commonly associated with stem canker diseases in woody plants of the *Rosaceae* family (Fan et al., 2020). In addition, *Cytospora sorbicola,* a species identified in *Prunus* species in California, has been linked to gummosis and tree decline, particularly in stressed fruit trees (Lawrence et al., 2018). Similarly, *B. dothidea* causes cankers and wood rot and is frequently detected in peach trees (Jo et al., 2022; Reilly, 1982; F. Wang et al., 2011).

Beyond the detection of *M. fruticola*, several other fungal pathogens known to affect leaves and fruit were also identified, including *Alternaria* spp. and *Botrytis cinerea*. *Alternaria* species are commonly associated with leaf spots, blights, and fruit rots in numerous crops, including fruit trees and vegetables. In woody tissues, *Alternaria* infections can cause leaf spots and, in severe cases, contribute to dieback (Florea & Puia, 2020). *B. cinerea*, the causative agent of grey mold, has an extensive host range, affecting economically important vegetables, fruits, and ornamental crops (Azevedo et al., 2020; Petrasch et al., 2019). This necrotrophic pathogen employs a suite of cell-wall-degrading enzymes, toxins, and low-molecular-weight compounds, such as botrydial, to facilitate host colonization (Kars & van Kan, 2007).

Notably, *Epicoccum nigrum* was also isolated. This species is naturally present in the mycobiota of peach twigs and flowers (Melgarejo et al., 1985), and has been widely studied for its biocontrol potential. *E. nigrum* has been used to manage peach twig blight caused by *M. laxa* (Melgarejo et al., 1986; Madrigal et al., 1994; Larena et al., 2005) and has demonstrated antagonistic activity against various plant pathogens (Christova & Slavov, 2021; T. Li et al., 2022). In our study, *E. nigrum* was isolated from symptomatic tissues in trees exhibiting signs such as flower necrosis, gummosis and shoot dieback. However, we did not record symptom severity systematically across trees and therefore cannot determine whether the presence of *E. nigrum* was associated with any phenotypic attenuation of disease. Its potential as a biocontrol agent in this system is thus proposed based on its known properties in other pathosystems, and further functional validation will be required to confirm its role under controlled conditions.

M. fruticula was not detected by ITS2 metabarcoding, yet its presence was confirmed from isolates via PCR amplification with ITS1 and ITS4 primers. This discrepancy suggests that ITS2 may not be the optimal primer for detecting this particular taxon within fungal communities, even though different primers typically yield comparable results as DNA metabarcodes (Blaalid et al., 2013; Tedersoo et al., 2022). This underscores the importance of employing complementary methods to ensure a more comprehensive characterization of fungal communities in *Prunus* trees. Furthermore, the detailed characterization of fungal communities using ITS2 metabarcoding holds promise as a diagnostic tool. By analyzing the overall community fingerprint or targeting specific taxa, this approach may facilitate the early

detection of shifts in fungal composition that signal changes in plant health. Such diagnostic capabilities could be invaluable for monitoring and managing diseases in *Prunus* trees.

A broader understanding of fungal community dynamics in *P. persica* orchards, encompassing both pathogenic and potentially beneficial species, is essential for improving disease management and enhancing resilience. The identification of multiple fungal pathogens highlights the need for early detection and integrated control strategies to minimize negative impacts on tree health and fruit production. Moreover, the presence of *E. nigrum* and its documented biocontrol potential suggests that leveraging naturally occurring antagonists could offer a sustainable approach to disease mitigation.

Conclusions

This study highlights the profound impact of *Monilinia fructicola* on the structure and function of fungal communities in *Prunus persica*. The pathogen not only alters microbial diversity but also disrupts ecological interactions and community stability, potentially reducing fungal network resilience and increasing disease susceptibility. Although no formal metric of dysbiosis exists for plant-associated fungal communities, our results suggest that *M. fructicola* acts as a driver of fungal dysbiosis, restructuring microbial networks and promoting opportunistic taxa while suppressing dominant members of the healthy mycobiota. The observed shifts in fungal primary lifestyles further indicate that the pathogen accelerates tissue decomposition and modifies the ecological balance of the mycobiota, potentially facilitating secondary infections by other pathogens. Network analysis supports the notion that *M. fructicola* weakens fungal community connectivity, leading to a fragmentation of microbial interactions. The reduction in network complexity, lower node connectivity, and increased modularity in infected samples suggest that the pathogen compromises ecological cohesion, favouring a more compartmentalized and less resilient fungal structure. The shift in dominant fungal genera, with the exclusion of previously abundant taxa and the emergence of pathogen-associated species, highlights the selective pressure exerted by *M. fructicola*, potentially favouring opportunistic or stress-adapted fungi.

In addition to high-throughput sequencing, the successful isolation and molecular identification of 19 fungal species from symptomatic tissues provide crucial insights into the pathogenic and beneficial fungal diversity within *P. persica* orchards. The identification of

multiple canker-causing fungi (*Diaporthe, Cytospora*, and *Botryosphaeria*) and major fruit pathogens (*M. fructicola* and *Botrytis cinerea*) underscores the complexity of fungal diseases affecting these trees. Importantly, the isolation of *Epicoccum nigrum*, a known biocontrol agent, suggests that naturally occurring antagonistic fungi could be leveraged for sustainable disease management. These isolates offer a unique opportunity for future functional studies, including pathogenicity assays, biocontrol screening, and microbiome-based disease management approaches.

Together, these findings reinforce the relevance of community-level fungal dynamics in plant health and disease. A deeper understanding of pathogen-induced shifts, particularly regarding host susceptibility, disease progression, and microbial-mediated defence mechanisms, may support the development of microbiome-informed strategies that provide sustainable alternatives to conventional disease control, integrating beneficial fungal isolates to enhance orchard resilience and productivity.

Acknowledgements

We sincerely thank the peach producers and the APPIZEZERE Producers Association for granting access to the orchards, which was essential for this study.

Funding

This research was funded by national funds through FCT - Fundação para a Ciência e a Tecnologia, I.P., under the project XylOut (DOI: 10.54499/PTDC/ASP-PLA/3145/2021). It was further supported by FCT - Fundação para a Ciência e Tecnologia, I.P., in the framework of the Project UIDB/04004/2025 - Centre for Functional Ecology - Science for the People & the Planet and LA/P/0092/2020: Associated Laboratory TERRA. Elsa Baltazar and Ricardo Leitão are the recipients of the fellowships UI/BD/150981/2021 and 2022.11630.BD from FCT, respectively. E. Garcia acknowledges support from the Interface Program – the core funding program of the Technology and Innovation Center, funded by the Recovery and Resilience Plan, under the terms of the Call for Proposals (AAC) No. 03/C05-i02/2022.

Literature Cited

Abarenkov, K., Nilsson, R. H., Larsson, K.-H., Taylor, A. F. S., May, T. W., Frøslev, T. G., Pawlowska, J., Lindahl, B., Põldmaa, K., Truong, C., Vu, D., Hosoya, T., Niskanen, T., Piirmann, T., Ivanov, F., Zirk, A., Peterson, M., Cheeke, T. E., Ishigami, Y., … Kõljalg, U. (2024). The UNITE database for molecular identification and taxonomic communication of fungi and other eukaryotes: Sequences, taxa and classifications reconsidered. *Nucleic Acids Research*, *52*(D1), D791–D797. https://doi.org/10.1093/nar/gkad1039

Ahmed, H. I., Herrera, M., Liew, Y. J., & Aranda, M. (2019). Long-Term Temperature Stress in the Coral Model Aiptasia Supports the "Anna Karenina Principle" for Bacterial Microbiomes. *Frontiers in Microbiology*, *10*. https://doi.org/10.3389/fmicb.2019.00975

Aleklett, K., Hart, M., & Shade, A. (2014). The microbial ecology of flowers: An emerging frontier in phyllosphere research. *Botany*, *92*(4), 253–266. https://doi.org/10.1139/cjb-2013-0166

Altschul, S. F., Gish, W., Miller, W., Myers, E. W., & Lipman, D. J. (1990). Basic local alignment search tool. *Journal of Molecular Biology*, *215*(3), Artigo 3. https://doi.org/10.1016/S0022-2836(05)80360-2

Arnault, G., Mony, C., & Vandenkoornhuyse, P. (2023). Plant microbiota dysbiosis and the Anna Karenina Principle. *Trends in Plant Science*, *28*(1), Artigo 1. https://doi.org/10.1016/j.tplants.2022.08.012

Azevedo, D. M. Q., Martins, S. D. S., Guterres, D. C., Martins, M. D., Araújo, L., Guimarães, L. M. S., Alfenas, A. C., & Furtado, G. Q. (2020). Diversity, prevalence and phylogenetic positioning of *Botrytis* species in Brazil. *Fungal Biology*, *124*(11), 940–957. https://doi.org/10.1016/j.funbio.2020.08.002

Baltazar, E., Rodrigues, S., Ares, A., Camelo, A., Brandão, I., Espirito Santo, C., Trovão, J., Garcia, E., & Costa, J. (2023). Morphological, Molecular and Genomic Identification and Characterisation of *Monilinia fructicola* in Prunus persica from Portugal. *Agronomy*, *13*(6), Artigo 6. https://doi.org/10.3390/agronomy13061493

Bez, C., Esposito, A., Thuy, H. D., Nguyen Hong, M., Valè, G., Licastro, D., Bertani, I., Piazza, S., & Venturi, V. (2021). The rice foot rot pathogen Dickeya zeae alters the in-field plant microbiome. *Environmental Microbiology*, *23*(12), 7671–7687. https://doi.org/10.1111/1462-2920.15726

Blaalid, R., Kumar, S., Nilsson, R. H., Abarenkov, K., Kirk, P. M., & Kauserud, H. (2013). ITS1 versus ITS2 as DNA metabarcodes for fungi. *Molecular Ecology Resources*, *13*(2), 218–224. https://doi.org/10.1111/1755-0998.12065

Bodenhausen, N., Bortfeld-Miller, M., Ackermann, M., & Vorholt, J. A. (2014). A Synthetic Community Approach Reveals Plant Genotypes Affecting the Phyllosphere Microbiota. *PLoS Genetics*, *10*(4), Artigo 4. https://doi.org/10.1371/journal.pgen.1004283

Bokulich, N. A., Kaehler, B. D., Rideout, J. R., Dillon, M., Bolyen, E., Knight, R., Huttley, G. A., & Gregory Caporaso, J. (2018). Optimizing taxonomic classification of marker-gene amplicon sequences with QIIME 2's q2-feature-classifier plugin. *Microbiome*, *6*(1), 90. https://doi.org/10.1186/s40168-018-0470-z

Bolyen, E., Rideout, J. R., Dillon, M. R., Bokulich, N. A., Abnet, C. C., Al-Ghalith, G. A., Alexander, H., Alm, E. J., Arumugam, M., Asnicar, F., Bai, Y., Bisanz, J. E., Bittinger, K., Brejnrod, A., Brislawn, C. J., Brown, C. T., Callahan, B. J., Caraballo-Rodríguez, A. M., Chase, J., … Caporaso, J. G. (2019). Reproducible, interactive, scalable and extensible microbiome data science using QIIME 2. *Nature Biotechnology*, *37*(8), 852–857. https://doi.org/10.1038/s41587-019-0209-9

Callahan, B. J., McMurdie, P. J., Rosen, M. J., Han, A. W., Johnson, A. J. A., & Holmes, S. P. (2016). DADA2: High-resolution sample inference from Illumina amplicon data. *Nature Methods*, *13*(7), 581–583. https://doi.org/10.1038/nmeth.3869

Casals, C., Torres, R., Teixidó, N., De Cal, A., Segarra, J., & Usall, J. (2022). Brown rot on stone fruit: From epidemiology studies to the development of effective control strategies. *Scientia Horticulturae*, *301*, 111096. https://doi.org/10.1016/j.scienta.2022.111096

Chen, T., Nomura, K., Wang, X., Sohrabi, R., Xu, J., Yao, L., Paasch, B. C., Ma, L., Kremer, J., Cheng, Y., Zhang, L., Wang, N., Wang, E., Xin, X.-F., & He, S. Y. (2020). A plant genetic network for preventing dysbiosis in the phyllosphere. *Nature*, *580*(7805), Artigo 7805. https://doi.org/10.1038/s41586-020-2185-0

Christova, P., & Slavov, S. (2021). Epicoccum nigrum -isolation, characterization and potential for biological control of *Botrytis cinerea*. *Bulgarian Journal of Agricultural Science*, *27*, 693–698.

Closek, C. J., Sunagawa, S., DeSalvo, M. K., Piceno, Y. M., DeSantis, T. Z., Brodie, E. L., Weber, M. X., Voolstra, C. R., Andersen, G. L., & Medina, M. (2014). Coral transcriptome and bacterial community profiles reveal distinct Yellow Band Disease states in *Orbicella faveolata*. *The ISME Journal*, *8*(12), 2411–2422. https://doi.org/10.1038/ismej.2014.85

Csárdi, G., & Nepusz, T. (2006). *The igraph software package for complex network research*. https://www.semanticscholar.org/paper/The-igraph-software-package-for-complex-network-Cs%C3%A1rdi-Nepusz/1d2744b83519657f5f2610698a8ddd177ced4f5c

Dubey, A., Malla, M. A., & Kumar, A. (2022). Role of Next-Generation Sequencing (NGS) in Understanding the Microbial Diversity. Em A. Kumar, B. Choudhury, S. Dayanandan, & M. L. Khan (Eds.), *Molecular Genetics and Genomics Tools in Biodiversity Conservation* (pp. 307–328). Springer Nature. https://doi.org/10.1007/978-981-16-6005-4_16

Eevers, N., Gielen, M., Sánchez-López, A., Jaspers, S., White, J. C., Vangronsveld, J., & Weyens, N. (2015). Optimization of isolation and cultivation of bacterial endophytes through addition of plant extract to nutrient media. *Microbial Biotechnology*, *8*(4), Artigo 4. https://doi.org/10.1111/1751-7915.12291

EPPO. (2019). *EPPO A1 and A2 Lists of Pests Recommended for Regulation as Quarantine Pests.* https://www.eppo.int/media/uploaded_images/ACTIVITIES/plant_quarantine/pm1-002-28-en.pdf

EPPO. (2020). PM 7/18 (3) *Monilinia fructicola*. *EPPO Bulletin*, *50*(1), Artigo 1. https://doi.org/10.1111/epp.12609

Fan, X. L., Bezerra, J. D. P., Tian, C. M., & Crous, P. W. (2020). Cytospora (Diaporthales) in China. *Persoonia : Molecular Phylogeny and Evolution of Fungi*, *45*, 1–45. https://doi.org/10.3767/persoonia.2020.45.01

FAOSTAT. (2023). https://www.fao.org/faostat/en/#data/QCL

FLOREA, A., & PUIA, C. (2020). Alternaria Genus and the Diseases Caused to Agricultural and Horticultural Plants. *Bulletin of University of Agricultural Sciences and Veterinary Medicine Cluj-Napoca. Agriculture*, *77*, 53. https://doi.org/10.15835/buasvmcn-agr:2020.0034

Harrell Jr, F. E. (2024). *Hmisc: Harrell Miscellaneous* (p. 5.2-1) [Dataset]. https://doi.org/10.32614/CRAN.package.Hmisc

Hortová, B., & Novotný, D. (2011). Endophytic fungi in branches of sour cherry trees: A preliminary study. *Czech Mycology*, *62*(1), 77–82. https://doi.org/10.33585/cmy.63107

J. P. Luz. (2014). *Diseases of Temperate Horticultural Plants* (George Raymond A. T. and Fox Roland T. V.). CABI.

Jo, Y., Jung, D.-R., Park, T.-H., Lee, D., Park, M.-K., Lim, K., & Shin, J.-H. (2022). Changes in Microbial Community Structure in Response to Gummosis in Peach Tree Bark. *Plants*, *11*(21), Artigo 21. https://doi.org/10.3390/plants11212834

Kars, I., & van Kan, J. A. L. (2007). Extracellular Enzymes and Metabolites Involved in Pathogenesis of *Botrytis*. Em Y. Elad, B. Williamson, P. Tudzynski, & N. Delen (Eds.), *Botrytis: Biology, Pathology and Control* (pp. 99–118). Springer Netherlands. https://doi.org/10.1007/978-1-4020-2626-3_7

Lahti, L., & Shetty, S. (2017). *Tools for microbiome analysis in R.* [R]. microbiome. https://github.com/microbiome/microbiome

Lamelas, A., Desgarennes, D., López-Lima, D., Villain, L., Alonso-Sánchez, A., Artacho, A., Latorre, A., Moya, A., & Carrión, G. (2020). The Bacterial Microbiome of Meloidogyne-Based

Disease Complex in Coffee and Tomato. *Frontiers in Plant Science*, *11*, 136. https://doi.org/10.3389/fpls.2020.00136

Larena, I., Torres, R., De Cal, A., Liñán, M., Melgarejo, P., Domenichini, P., Bellini, A., Mandrin, J. F., Lichou, J., de Eribe, X. O., & Usall, J. (2005). Biological control of postharvest brown rot (*Monilinia* spp.) of peaches by field applications of *Epicoccum nigrum*. *Biological Control*, *32*(2), 305–310. https://doi.org/10.1016/j.biocontrol.2004.10.010

Lawrence, D. P., Holland, L. A., Nouri, M. T., Travadon, R., Abramians, A., Michailides, T. J., & Trouillas, F. P. (2018). Molecular phylogeny of Cytospora species associated with canker diseases of fruit and nut crops in California, with the descriptions of ten new species and one new combination. *IMA Fungus*, *9*, 333–370. https://doi.org/10.5598/imafungus.2018.09.02.07

Layeghifard, M., Hwang, D. M., & Guttman, D. S. (2018). Constructing and Analyzing Microbiome Networks in R. Em R. G. Beiko, W. Hsiao, & J. Parkinson (Eds.), *Microbiome Analysis: Methods and Protocols* (pp. 243–266). Springer. https://doi.org/10.1007/978-1-4939-8728-3_16

Li, H.-L. (1978). *The Domestication of Plants in China: Ecogeographical Considerations*. Conference on the origins of Chinese Civilization.

Li, T., Im, J., & Lee, J. (2022). Genetic Diversity of Epicoccum nigrum and its Effects on Fusarium graminearum. *Mycobiology*, *50*(6), 457–466. https://doi.org/10.1080/12298093.2022.2148394

Liao, X., Greenspan, P., & Pegg, R. B. (2019). Characterizing the phenolic constituents and antioxidant capacity of Georgia peaches. *Food Chemistry*, *271*, 345–353. https://doi.org/10.1016/j.foodchem.2018.07.163

Linlin, Y. (2023). *ggvenn: Draw Venn Diagram by «ggplot2»* (Versão 0.1.10) [Software]. https://cran.r-project.org/web/packages/ggvenn/index.html

Love, M. I., Huber, W., & Anders, S. (2014). Moderated estimation of fold change and dispersion for RNA-seq data with DESeq2. *Genome Biology*, *15*(12), 550. https://doi.org/10.1186/s13059-014-0550-8

Lozupone, C. A., Stombaugh, J. I., Gordon, J. I., Jansson, J. K., & Knight, R. (2012). Diversity, stability and resilience of the human gut microbiota. *Nature*, *489*(7415), 220–230. https://doi.org/10.1038/nature11550

Luo, C.-X., Schnabel, G., Hu, M., & De Cal, A. (2022). Global distribution and management of peach diseases. *Phytopathology Research*, *4*(1), Artigo 1. https://doi.org/10.1186/s42483-022-00134-0

Ma, Z. (Sam). (2020). Testing the Anna Karenina Principle in Human Microbiome-Associated Diseases. *iScience*, *23*(4), Artigo 4. https://doi.org/10.1016/j.isci.2020.101007

Ma, Z. (Sam), Li, L., & Gotelli, N. J. (2019). Diversity-disease relationships and shared species analyses for human microbiome-associated diseases. *The ISME Journal*, *13*(8), 1911–1919. https://doi.org/10.1038/s41396-019-0395-y

Madrigal, C., Pascual, S., & Melgarejo, P. (1994). Biological control of peach twig blight (*Monilinia laxa*) with Epicoccum nigrum. *Plant Pathology*, *43*(3), 554–561. https://doi.org/10.1111/j.1365-3059.1994.tb01590.x

Martini, C., & Mari, M. (2014). *Monilinia fructicola*, *Monilinia laxa* (Monilinia Rot, Brown Rot). Em S. Bautista-Baños (Ed.), *Postharvest Decay* (pp. 233–265). Academic Press. https://doi.org/10.1016/B978-0-12-411552-1.00007-7

McMurdie, P. J., & Holmes, S. (2013). phyloseq: An R Package for Reproducible Interactive Analysis and Graphics of Microbiome Census Data. *PLOS ONE*, *8*(4), e61217. https://doi.org/10.1371/journal.pone.0061217

Melgarejo, P., Carrillo, R., & Sagasta, E. M. (1985). Mycoflora of peach twigs and flowers and its possible significance in biological control of *Monilinia laxa*. *Transactions of the British Mycological Society*, *85*(2), 313–317. https://doi.org/10.1016/S0007-1536(85)80194-7

Melgarejo, P., Carrillo, R., & -Sagasta, E. M. (1986). Potential for biological control of *Monilinia laxa* in peach twigs. *Crop Protection*, *5*(6), 422–426. https://doi.org/10.1016/0261-2194(86)90076-1

Müller, D. B., Vogel, C., Bai, Y., & Vorholt, J. A. (2016). The Plant Microbiota: Systems-Level Insights and Perspectives. *Annual Review of Genetics*, *50*(1), 211–234. https://doi.org/10.1146/annurev-genet-120215-034952

Nian, L., Xie, Y., Zhang, H., Wang, M., Yuan, B., Cheng, S., & Cao, C. (2023). *Vishniacozyma victoriae*: An endophytic antagonist yeast of kiwifruit with biocontrol effect to *Botrytis cinerea*. *Food Chemistry*, *411*, 135442. https://doi.org/10.1016/j.foodchem.2023.135442

Oksanen, J., Simpson, G. L., Blanchet, F. G., Kindt, R., Legendre, P., Minchin, P. R., O'Hara, R. B., Solymos, P., Stevens, M. H. H., Szoecs, E., Wagner, H., Barbour, M., Bedward, M., Bolker, B., Borcard, D., Carvalho, G., Chirico, M., Caceres, M. D., Durand, S., … Weedon, J. (2024). *vegan: Community Ecology Package* (Versão 2.6-8) [Software]. https://cran.r-project.org/web/packages/vegan/index.html

Pakbin, B., Razavi, S. H., Mahmoudi, R., & Gajarbeygi, P. (2014). Producing Probiotic Peach Juice. *Biotechnology and Health Sciences*, *1*(3), Artigo 3. https://doi.org/10.17795/bhs-24683

Pedersen, T. L. (2024). *ggraph: An Implementation of Grammar of Graphics for Graphs and Networks* (Versão 2.2.1) [Software]. https://cran.r-project.org/web/packages/ggraph/index.html

Petrasch, S., Knapp, S. J., van Kan, J. A. L., & Blanco-Ulate, B. (2019). Grey mould of strawberry, a devastating disease caused by the ubiquitous necrotrophic fungal pathogen Botrytis cinerea. *Molecular Plant Pathology*, *20*(6), 877–892. https://doi.org/10.1111/mpp.12794

Põlme, S., Abarenkov, K., Henrik Nilsson, R., Lindahl, B. D., Clemmensen, K. E., Kauserud, H., Nguyen, N., Kjøller, R., Bates, S. T., Baldrian, P., Frøslev, T. G., Adojaan, K., Vizzini, A., Suija, A., Pfister, D., Baral, H.-O., Järv, H., Madrid, H., Nordén, J., … Tedersoo, L. (2020).

FungalTraits: A user-friendly traits database of fungi and fungus-like stramenopiles. *Fungal Diversity*, *105*(1), 1–16. https://doi.org/10.1007/s13225-020-00466-2

Portal do INE. (2020). Estatisticas Agricolas. https://www.ine.pt/xportal/xmain?xpid=INE&xpgid=ine_publicacoes&PUBLICACOESpub_boui=437147278&PUBLICACOEStema=55505&PUBLICACOESmodo=2

Reilly, C. C. (1982). Distribution in the Southeastern United States of Peach Tree Fungal Gummosis Caused by *Botryosphaeria dothidea*. *Plant Disease*, *66*(1), 158. https://doi.org/10.1094/PD-66-158

Rivers, A. R., Weber, K. C., Gardner, T. G., Liu, S., & Armstrong, S. D. (2018). *ITSxpress: Software to rapidly trim internally transcribed spacer sequences with quality scores for marker gene analysis* (No. 7:1418). F1000Research. https://doi.org/10.12688/f1000research.15704.1

Sisquella, M., Viñas, I., Picouet, P., Torres, R., & Usall, J. (2014). Effect of host and *Monilinia* spp. Variables on the efficacy of radio frequency treatment on peaches. *Postharvest Biology and Technology*, *87*, 6–12. https://doi.org/10.1016/j.postharvbio.2013.07.042

Sun, X., & Guo, L.-D. (2012). Endophytic fungal diversity: Review of traditional and molecular techniques. *Mycology*, *3*(1), 65–76. https://doi.org/10.1080/21501203.2012.656724

Tanunchai, B., Ji, L., Schroeter, S. A., Wahdan, S. F. M., Hossen, S., Delelegn, Y., Buscot, F., Lehnert, A.-S., Alves, E. G., Hilke, I., Gleixner, G., Schulze, E.-D., Noll, M., & Purahong, W. (2023). FungalTraits vs. FUNGuild: Comparison of Ecological Functional Assignments of Leaf- and Needle-Associated Fungi Across 12 Temperate Tree Species. *Microbial Ecology*, *85*(2), 411–428. https://doi.org/10.1007/s00248-022-01973-2

Team, R. C. (2024). *_R: A Language and Environment for Statistical Computing_*. R: The R Project for Statistical Computing. https://www.r-project.org/

Tedersoo, L., Bahram, M., Zinger, L., Nilsson, R. H., Kennedy, P. G., Yang, T., Anslan, S., & Mikryukov, V. (2022). Best practices in metabarcoding of fungi: From experimental design to results. *Molecular Ecology*, *31*(10), 2769–2795. https://doi.org/10.1111/mec.16460

Thangaraj, P., Muthusamy, N., & Seethapathy, P. (2025). Taphrina. Em N. Amaresan & K. Kumar (Eds.), *Compendium of Phytopathogenic Microbes in Agro-Ecology: Vol.1 Fungi* (pp. 837–854). Springer Nature Switzerland. https://doi.org/10.1007/978-3-031-81770-0_35

Thompson, S. M., Tan, Y. P., Young, A. J., Neate, S. M., Aitken, E. A. B., & Shivas, R. G. (2011). Stem cankers on sunflower (Helianthus annuus) in Australia reveal a complex of pathogenic Diaporthe (Phomopsis) species. *Persoonia : Molecular Phylogeny and Evolution of Fungi*, *27*, 80–89. https://doi.org/10.3767/003158511X617110

Thukral, A. (2017). A review on measurement of Alpha diversity in biology. *Agricultural Research Journal*, *54*, 1. https://doi.org/10.5958/2395-146X.2017.00001.1

Van Brouwershaven, I. R., Bruil, M. L., Van Leeuwen, G. C. M., & Kox, L. F. F. (2010). A real-time (TaqMan) PCR assay to differentiate *Monilinia fructicola* from other brown rot fungi of fruit crops. *Plant Pathology*, *59*(3), 548–555. https://doi.org/10.1111/j.1365-3059.2009.02220.x

Vandenkoornhuyse, P., Quaiser, A., Duhamel, M., Le Van, A., & Dufresne, A. (2015). The importance of the microbiome of the plant holobiont. *New Phytologist*, *206*(4), Artigo 4. https://doi.org/10.1111/nph.13312

Vannier, N., Mony, C., Bittebière, A.-K., & Vandenkoornhuyse, P. (2015). Epigenetic Mechanisms and Microbiota as a Toolbox for Plant Phenotypic Adjustment to Environment. *Frontiers in Plant Science*, *6*. https://doi.org/10.3389/fpls.2015.01159

Vorholt, J. A. (2012). Microbial life in the phyllosphere. *Nature Reviews Microbiology*, *10*(12), Artigo 12. https://doi.org/10.1038/nrmicro2910

Wang, F., Zhao, L., Li, G., Huang, J., & Hsiang, T. (2011). Identification and Characterization of Botryosphaeria spp. Causing Gummosis of Peach Trees in Hubei Province, Central China. *Plant Disease*, *95*(11), 1378–1384. https://doi.org/10.1094/PDIS-12-10-0893

Wang, H., Guo, S., Huang, M., Thorsten, L. H., & Wei, J. (2010). Ascomycota has a faster evolutionary rate and higher species diversity than Basidiomycota. *Science China Life Sciences*, *53*(10), 1163–1169. https://doi.org/10.1007/s11427-010-4063-8

White, T. J., Bruns, T., Lee, S., & Taylor, J. (1990). Amplification and direct sequencing of fungal ribosomal RNA genes for phylogenetics. In *PCR Protocols* (pp. 315–322). Elsevier. https://doi.org/10.1016/B978-0-12-372180-8.50042-1

Wickham, H. (2016). *Ggplot2*. Springer International Publishing. https://doi.org/10.1007/978-3-319-24277-4

Zaneveld, J. R., McMinds, R., & Vega Thurber, R. (2017). Stress and stability: Applying the Anna Karenina principle to animal microbiomes. *Nature Microbiology*, *2*(9), Artigo 9. https://doi.org/10.1038/nmicrobiol.2017.121

Zhang, M., Kong, Z., Fu, H., Shu, X., Xue, Q., Lai, H., & Guo, Q. (2023). Rhizosphere microbial ecological characteristics of strawberry root rot. *Frontiers in Microbiology*, *14*, 1286740. https://doi.org/10.3389/fmicb.2023.1286740

Zheng, Y., Crawford, G. W., & Chen, X. (2014). Archaeological Evidence for Peach (Prunus persica) Cultivation and Domestication in China. *PLOS ONE*, *9*(9), Artigo 9. https://doi.org/10.1371/journal.pone.0106595

Zheng, Y., Wang, J., Zhao, W., Cai, X., Xu, Y., Chen, X., Yang, M., Huang, F., Yu, L., & He, Y. (2022). Effect of Bacterial Wilt on Fungal Community Composition in Rhizosphere Soil of Tobaccos in Tropical Yunnan. *The Plant Pathology Journal*, *38*(3), 203–211. https://doi.org/10.5423/PPJ.OA.03.2022.0035

Zhou, Y., Zhang, W., Abeywickrama, P. D., He, Z., Zhang, Z., Li, Y., Li, S., Fan, Z., & Yan, J. (2024). Diversity and Virulence of Diaporthe Species Associated with Peach Trunk Diseases in China. *Plants*, *13*(22), Artigo 22. https://doi.org/10.3390/plants13223238

a)

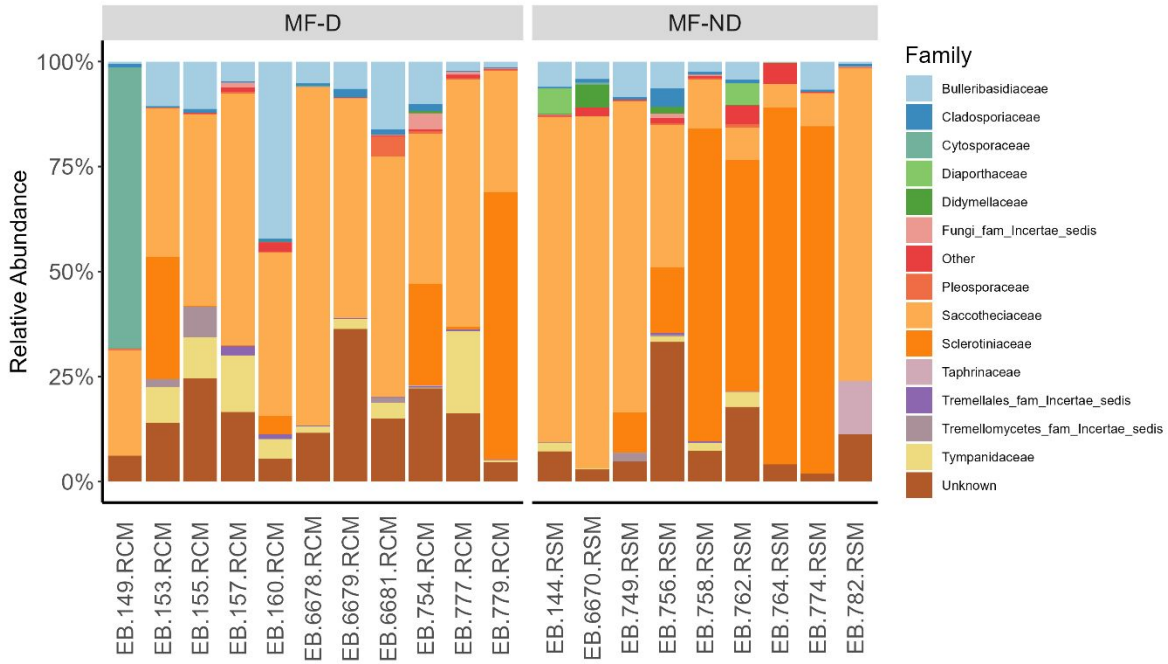

b)

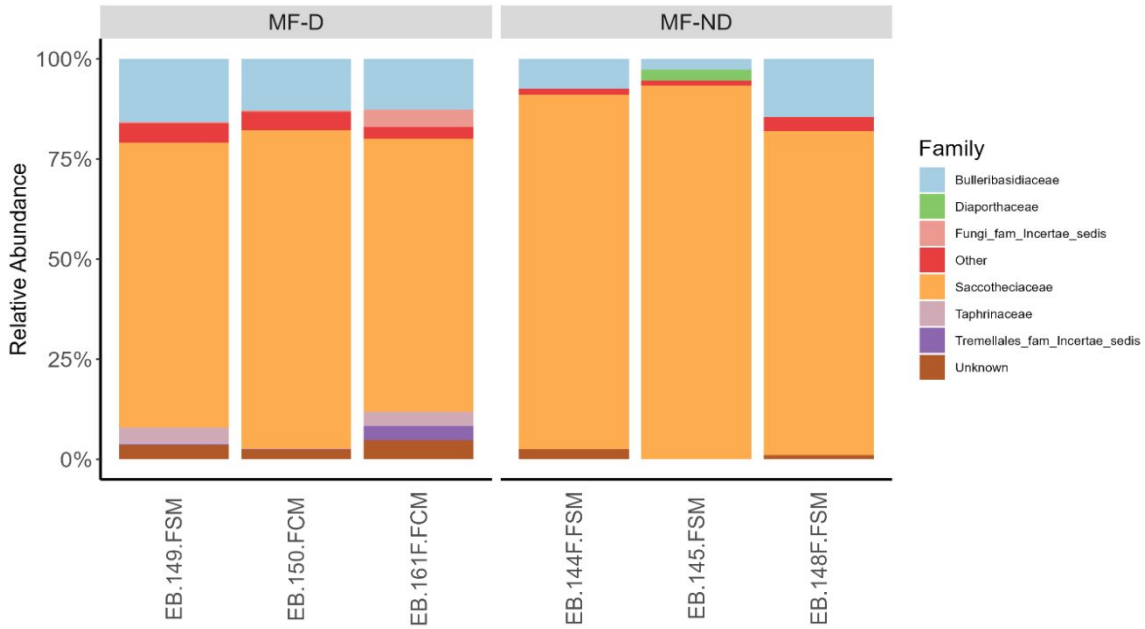

Figure 1- Taxonomic composition of fungal communities at the family level. The bar plots display the relative abundance of fungal families in (a) wood and (b) flowers, categorized by the absence (MF-ND) and presence (MF-D) of *Monilinia fructicola*. Families with a relative abundance below 2% across all samples were grouped into the "Other" category.

a) **b)**

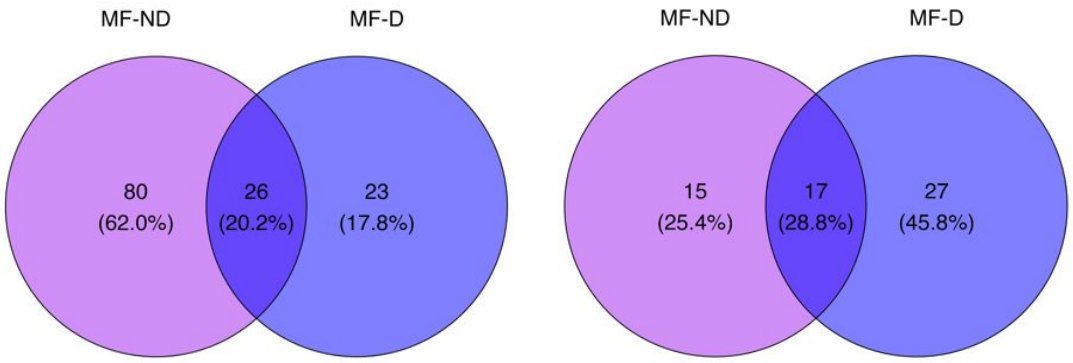

Figure 2 - Venn diagrams showing the shared and unique fungal genera in (a) wood and (b) flower samples, based on the absence (MF-ND) and presence (MF-D) of *Monilinia fructicola.*

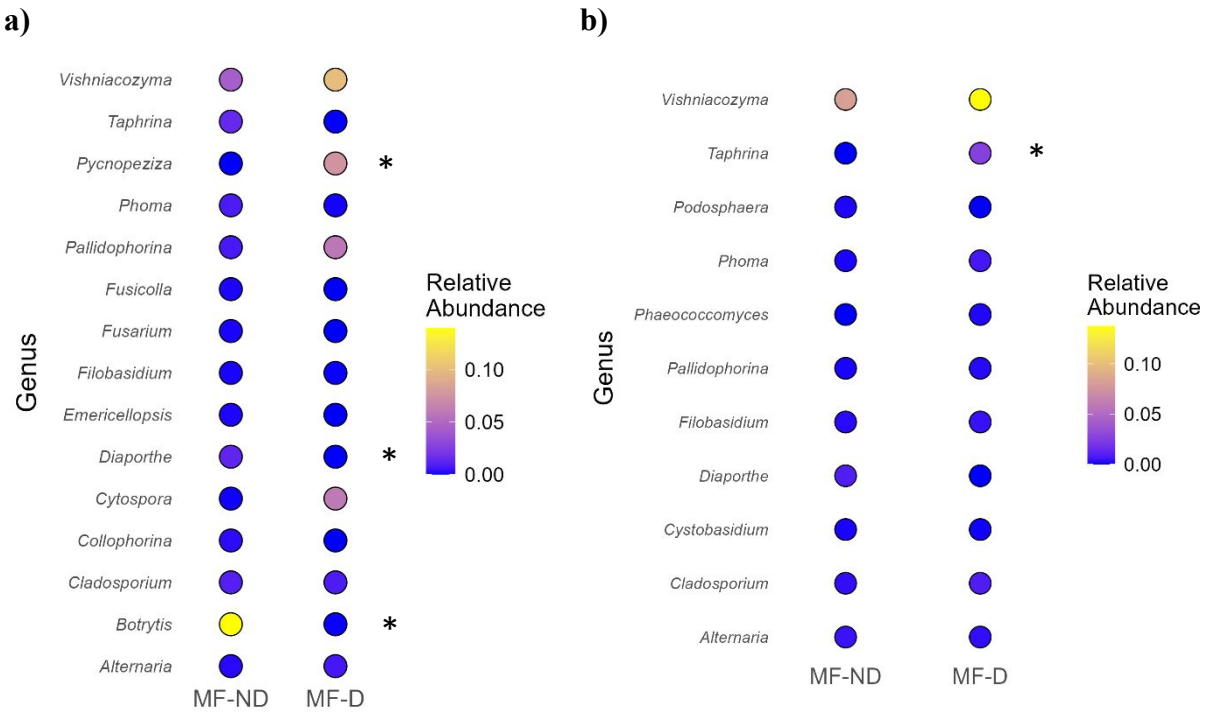

Figure 3. Heatmap of relative abundances of fungal genera in (a) wood and (b) flower samples based on the absence (MF-ND) and presence (MF-D) of *Monilinia fructicola*. To improve visibility, the highly dominant genus *Aureobasidium* and unknown/unidentified genera were excluded. Genera with relative abundances below 0.1% were also removed. The colour gradient represents relative abundance, with yellow indicating higher abundance and blue indicating lower abundance. Rows correspond to fungal genera, while columns represent the *M. fructicola* detection group.

a)

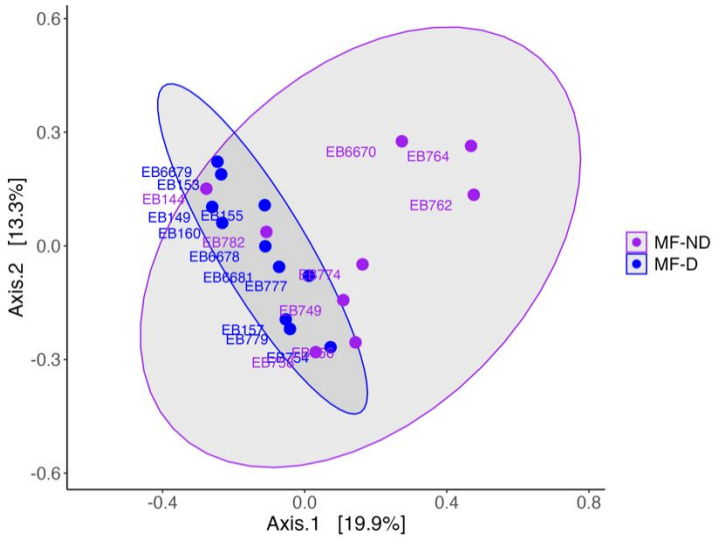

b)

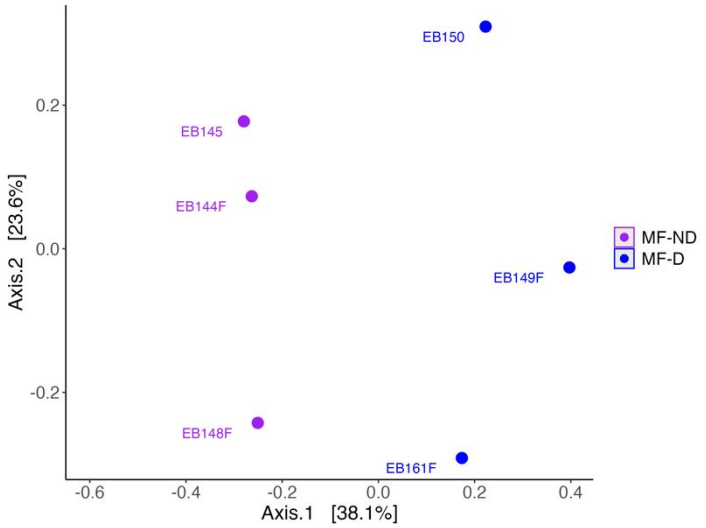

Figure 4 - Principal Coordinate Analysis (PCoA) of fungal communities based on UniFrac distances in (a) wood and (b) flower samples, categorized by the absence (MF-ND) and presence (MF-D) of *Monilinia fructicola*. Each point represents a single sample labelled by its corresponding sample name. The proximity between points reflects the similarity of fungal community composition, with closer points indicating more similar communities. Axis 1 and Axis 2 denote the variance explained by the first two principal coordinates.

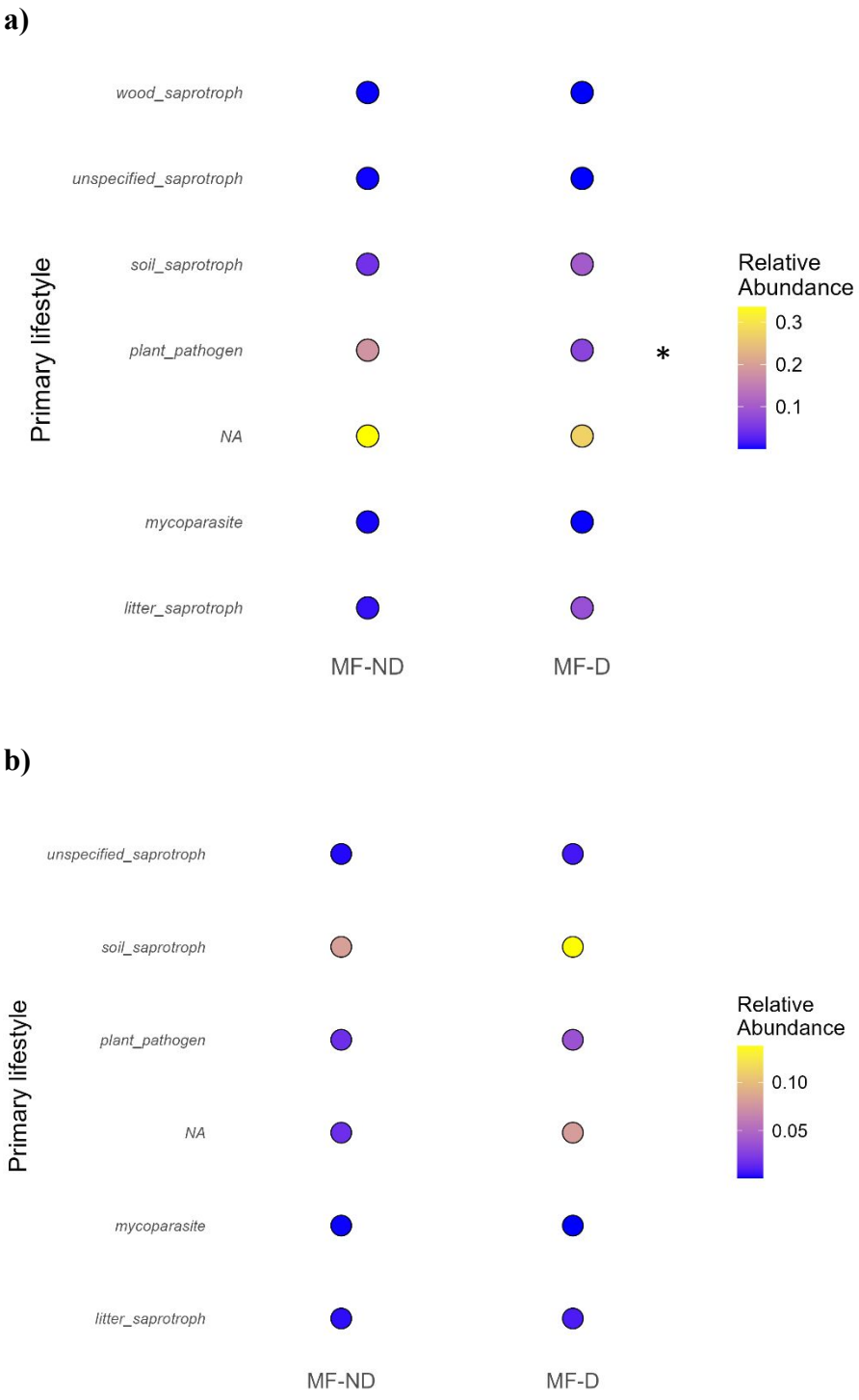

Figure 5. Heatmap of relative abundances of fungal primary lifestyles in (a) wood and (b) flower samples, categorized by the absence (MF-ND) and presence (MF-D) of *Monilinia fructicola*, extracted using FungalTraits. To improve visibility, the group Sooty mold, which was highly dominant and had slight differences in abundance between MF-ND and MF-D was excluded. Groups with relative abundances below 0.1% were also removed. The colour gradient represents relative abundance, with yellow indicating higher abundance and blue indicating lower abundance. Rows correspond to primary lifestyle groups while columns represent detection groups.

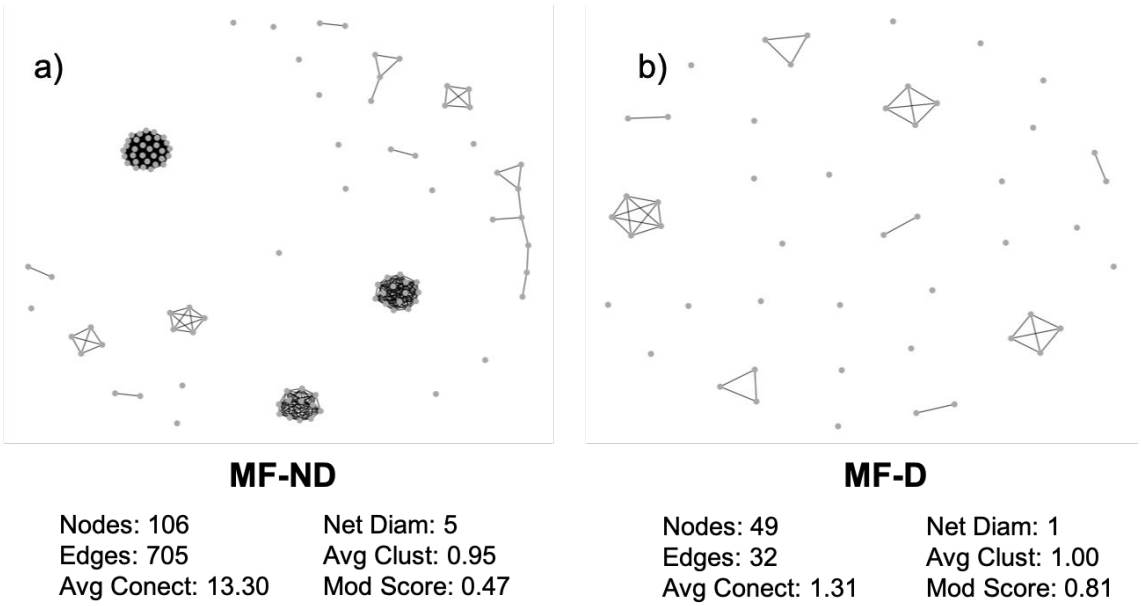

Figure 6. Wood fungal co-occurrence networks at the genus level in the (a) absence (MF-ND) and (b) presence (MF-D) of *Monilinia fructicola*. Below each network, values are provided for the number of nodes, number of edges, average node connectivity, network diameter, average clustering coefficient, and modularity score. The networks represent genus-level associations and are intended to highlight structural differences in community connectivity under contrasting conditions.

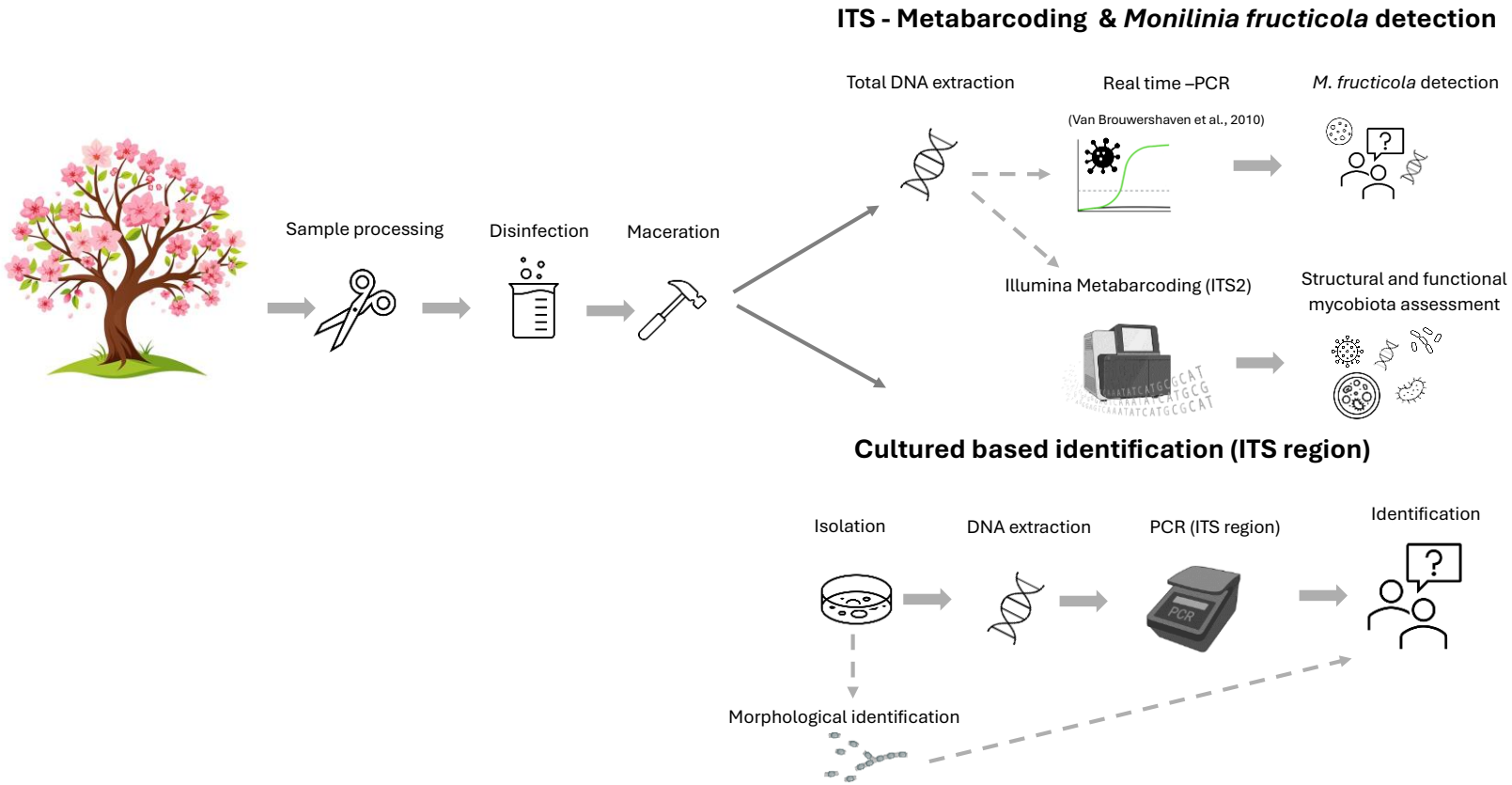

Supplementary Figure S1 - Overview of the experimental workflow combining culture-dependent and culture-independent approaches to assess the impact of *Monilinia fructicola* on the fungal community of *Prunus persica*.

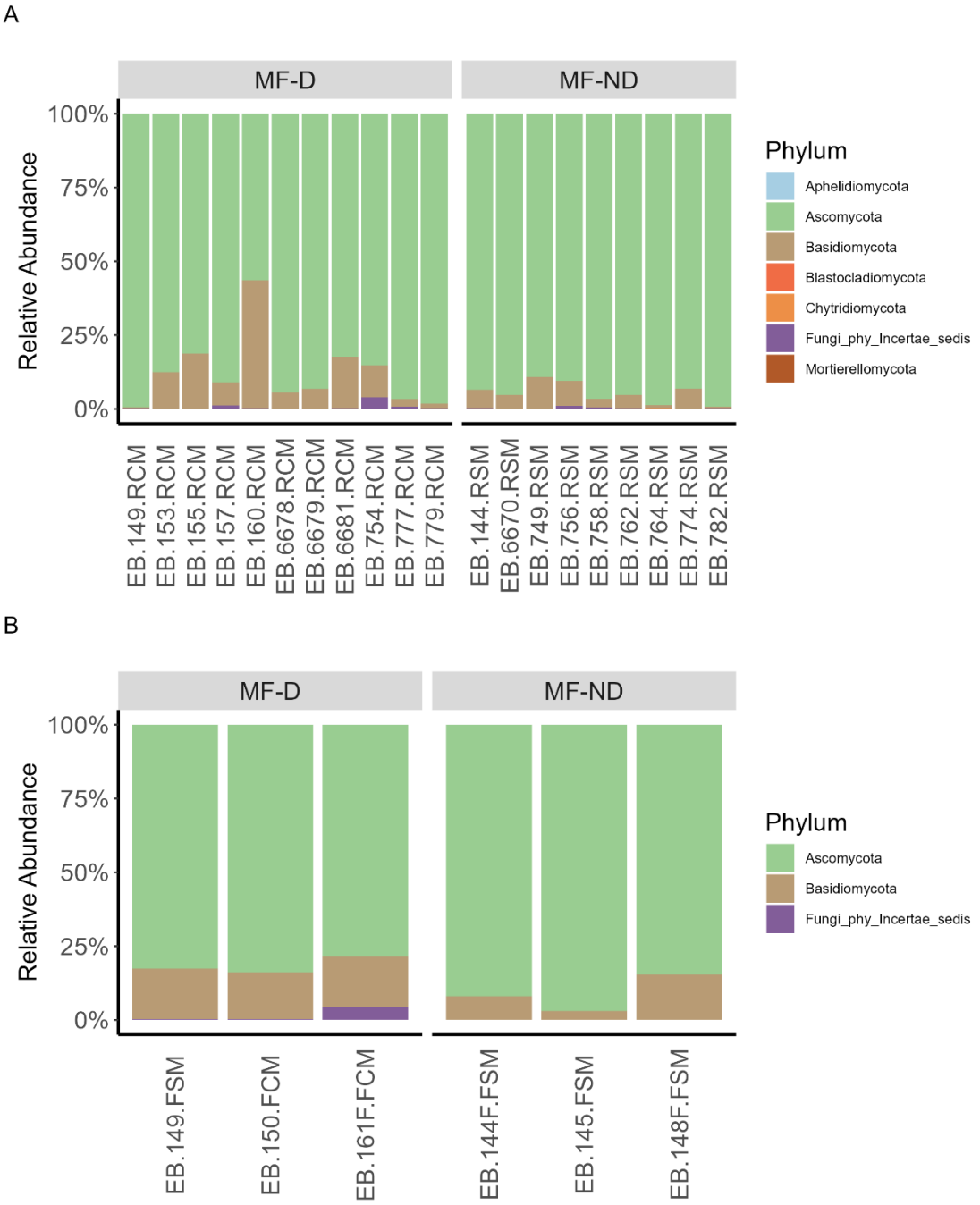

Supp1ementary Figure S2- Taxonomic composition of fungal communities at the phylum level. The bar plots display the relative abundance of fungal families in (a) wood and (b) flowers, categorized by the absence (MF-ND) and presence (MF-D) of *Monilinia fructicola*. Phyla with a relative abundance below 1% across all samples were grouped into the "Other" category.

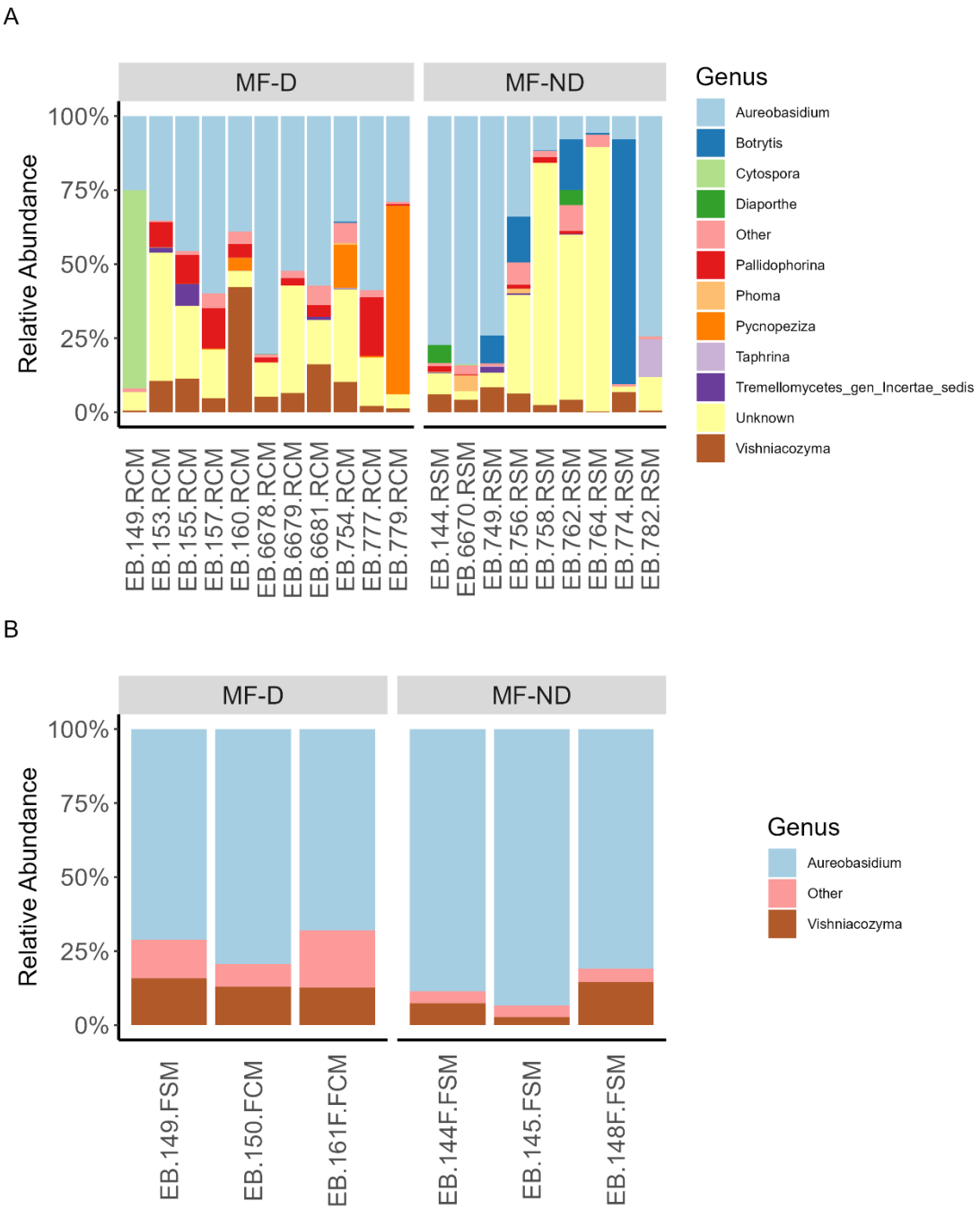

Supp1ementary Figure S3- Taxonomic composition of fungal communities at the genus level. The bar plots display the relative abundance of fungal families in (a) wood and (b) flowers, categorized by the absence (MF-ND) and presence (MF-D) of *Monilinia fructicola*. Genus with a relative abundance below 2% across all samples were grouped into the "Other" category.

a)

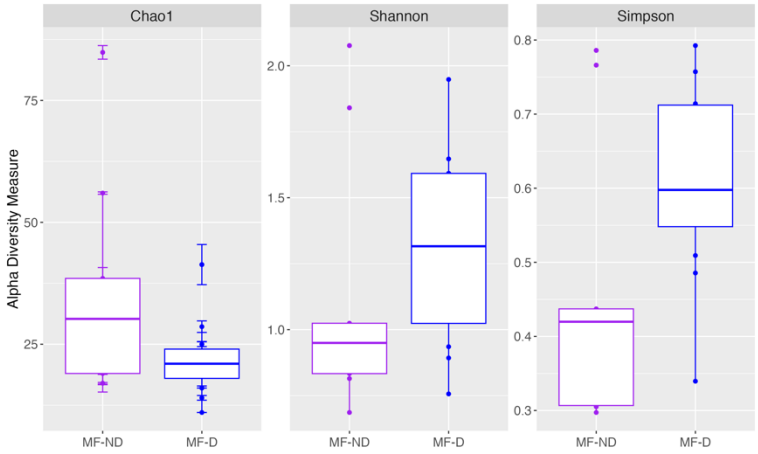

b)

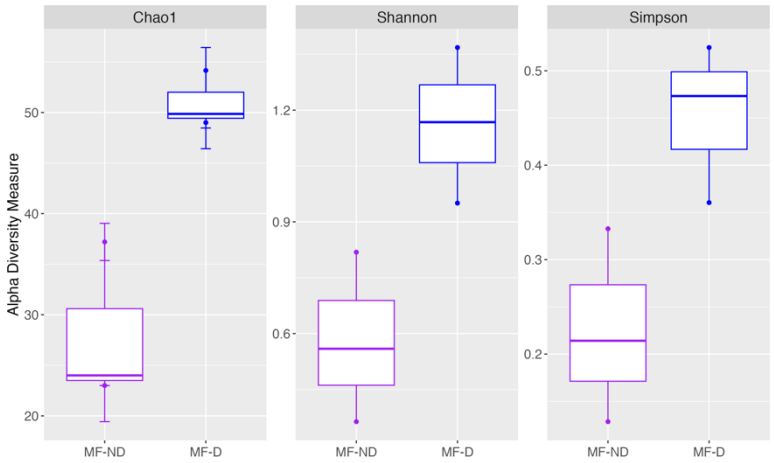

Supp1ementary Figure S4 - Alpha diversity indices (Chao1, Shannon, and Simpson) for fungal communities in (a) wood samples and (b) flower samples. The boxplots represent the distribution of alpha diversity indices across the absence (MF-ND) and the presence (MF-D) of *M. fructicola*, highlighting differences in fungal community richness and diversity.

Supplementary Table 1 - Localization of the sampled orchards, type of plant material collected, and fungal detection approaches. NGS metabarcoding was used for general fungal screening, ITS conventional PCR for fungal isolation and identification, and RT-PCR (EPPO protocol) for *Monilinia fructicola* confirmation.

Orchard	Localization	Sample	Material	NGS Metabarcoding	ITS Conventional PCR	EPPO Detection (RT-PCR)
P1	Solheira	**EB_144**	Wood	x	x	
		EB_144F	Flower	x		
		EB_145	Flower	x		
P2	Atalaia do Campo	**EB_148**	Wood	x	x	
		EB_148F	Flower	x		
		EB_149	Wood	x	x	
		EB_149F	Flower	x		
		EB_150	Flower	x		
P3	Inguias	**EB_153**	Wood	x	x	
		EB_155	Wood	x	x	x
		EB_775	Wood	x	x	
		EB_6678	Wood	x		
		EB_6679	Wood	x		
		EB_6681	Wood	x		
P4	Colmeal da Torre	**EB_157**	Wood	x	x	x
		EB_160	Wood	x	x	x
		EB_161F	Flower	x		x
		EB_777	Wood	x		
P5	Borralheira	**EB_779**	Wood	x	x	x
		EB_749	Wood	x		
P6	Teixoso	**EB_753**	Wood	x	x	x
P7	Orjais	**EB_754**	Wood	x	x	x
P8	Orjais	**EB_756**	Wood	x	x	
P9	Catraia da Torre	**EB_758**	Wood	x	x	
		EB_760	Wood	x		
P10	Carvalhal Formoso	**EB_762**	Wood	x	x	
P11	Carvalhal Formoso	**EB_764**	Wood	x	x	
		EB_772	Wood	x	x	
P12	Carvalhal Formoso	**EB_766**	Wood	x	x	
P13	Borralheira	**EB_774**	Wood	x	x	
		EB_782	Wood	x	x	
P14	Vale Formoso	**EB_6670**	Wood	x		

Supplementary Table S2 – Summary of QIIME2 pipeline outputs for each sample, including input reads, number of reads after filtering, percentage of input reads that passed filtering, denoised reads, merged reads, percentage of input reads successfully merged, non-chimeric reads, and percentage of input reads identified as non-chimeric. A blank control sample (EB.control) was also included in the analysis

sample-id	input	filtered	percentage of input passed filter	denoised	merged	percentage of input merged	non-chimeric	percentage of input non-chimeric
EB.144.RSM	17238	16324	94,7	16296	16171	93,81	15981	92,71
EB.144F.FSM	31434	31027	98,71	30980	30422	96,78	29581	94,11
EB.145.FSM	17983	17572	97,71	17535	17182	95,55	16988	94,47
EB.148.RSM	6151	6077	98,8	6058	5832	94,81	5784	94,03
EB.148F.FSM	29121	28791	98,87	28716	28299	97,18	27847	95,63
EB.149.FSM	30906	30578	98,94	30458	29909	96,77	29390	95,09
EB.149.RCM	14673	14458	98,53	14421	14159	96,5	13783	93,93
EB.150.FCM	38609	38197	98,93	38153	37938	98,26	37853	98,04
EB.153.RCM	24477	24231	98,99	24199	23936	97,79	22183	90,63
EB.155.RCM	43077	42605	98,9	42571	42268	98,12	39069	90,7
EB.157.RCM	18323	18174	99,19	18129	18013	98,31	16767	91,51
EB.160.RCM	51054	50495	98,91	50436	50261	98,45	49354	96,67
EB.161F.FCM	28679	28358	98,88	28279	27754	96,77	26640	92,89
EB.6670.RSM	43148	42506	98,51	42478	42235	97,88	42127	97,63
EB.6678.RCM	32566	32160	98,75	32112	32011	98,3	31515	96,77
EB.6679.RCM	50032	49438	98,81	49388	49228	98,39	48396	96,73
EB.6681.RCM	63466	62651	98,72	62631	62433	98,37	61611	97,08
EB.749.RSM	58903	58399	99,14	58350	58206	98,82	57750	98,04
EB.753.RCM	12505	10703	85,59	10690	10487	83,86	10388	83,07
EB.754.RCM	51175	50694	99,06	50633	50255	98,2	43418	84,84
EB.756.RSM	45388	44959	99,05	44889	44739	98,57	44179	97,34
EB.758.RSM	55380	54730	98,83	54707	54544	98,49	54041	97,58
EB.760.RSM	49865	49366	99	49001	47604	95,47	43802	87,84
EB.762.RSM	60222	57401	95,32	57263	56689	94,13	54684	90,8
EB.764.RSM	56886	56102	98,62	55955	55753	98,01	55490	97,55
EB.766.RSM	50012	49434	98,84	49049	47864	95,71	44861	89,7
EB.772.RSM	6828	6091	89,21	6071	5842	85,56	5800	84,94
EB.774.RSM	16614	16363	98,49	16355	16226	97,66	16149	97,2
EB.775.RSM	8917	8734	97,95	8699	8510	95,44	8403	94,24
EB.777.RCM	34297	33933	98,94	33899	33750	98,41	32005	93,32
EB.779.RCM	22525	22276	98,89	22244	22062	97,94	21806	96,81
EB.782.RSM	22601	22392	99,08	22358	22139	97,96	21970	97,21
EB.control	57015	56399	98,92	56110	55179	96,78	54414	95,44

Baltazar et al., Phytopathology

Supplementary Table S2 - Relative abundance of fungal genera detected in each sample and the respective taxonomic assignment.

kingdom	Phylum	Class	Order	Family	Genus	total_reads	n_ASVs	EB.144	EB.144F	EB.345	EB.348F	EB.349	EB.349	EB.350	EB.353	EB.355	EB.357	EB.360	EB.361F	EB.6670	EB.6678	EB.6679	EB.6681	EB.749	EB.754	EB.756	EB.758	EB.762	EB.764	EB.774	EB.777	EB.779	EB.782
	Aphelidiomycota	Aphelidiomycetes	GS16	GS16_fam_Incertae_sedis	GS16_gen_Incertae_sedis	13	1	0	0	0	0	0	0	0	0	0	0	0	0	0.00137513	0	0	0	0	0	0	0	0	0	0	0	0	0
	Ascomycota	Arthoniomycetes	Lichenostigmatales	Phaeococcomycetaceae	Phaeococcomycetes	92	4	0	0	0	0	0.424564064	0	0	0	0	0	0	0.053070508	0.219863533	0	0	0	0	0	0	0	0	0	0	0	0	0
		Ascomycota	Ascomycota	Ascomycota	Ascomycota	36043	12	7.187263078	2.680836391	0	1.053828658	3.623957544	6.133443442	2.585201888	14.02677771	24.56868819	16.42911296	5.542077331	4.549906682	3.297952995	12.13040182	36.16376042	14.72327521	4.882486732	21.74374526	30.11372252	7.831690675	17.15693707	3.995451099	1.063688795	15.71645186	4.154662623	11.06141016
		Ascomycota_cls_Incertae_sedis	Ascomycota_ord_Incertae_sedis	Ascomycota_fam_Incertae_sedis	Ascomycota_gen_Incertae_sedis	138	2	0.004540907	0	0	0	0	0.037907506	0	0.051634002	0.051634002	0.011722517	0.025089538	0.503260845	0	0	0	0	0	0	0	0	0	0	0	0.037907506	0	0.227628252	0
			Botryosphaeriales		Neofusicoccum	5	1	0	0	0.037907506	0	0	0	0	0	0	0	0	0	0	0	0	0	0	0	0	0	0	0	0	0	0	0
					Spencermartinsia	1	1	0	0	0	0	0	0	0	0	0.007581501	0	0	0	0	0	0	0	0	0	0	0	0	0	0	0	0	0	0
				Botryosphaeriales_fam_Incertae_sedis	Botryosphaeriales_gen_Incertae_sedis	5	1	0	0	0	0.037907506	0	0	0	0	0	0	0	0	0	0	0	0	0	0	0	0	0	0	0	0	0	0	0
			Capnodiales	Capnodiales_fam_Incertae_sedis	Capnodiales_gen_Incertae_sedis	1	1	0	0	0	0	0	0	0	0	0.007581501	0	0	0	0	0	0	0	0	0	0	0	0	0	0	0	0	0
			Cladosporiales	Cladosporiaceae	Cladosporium	2808	1	0.386665658	0.204700531	0.144048522	0.659590599	1.372521706	0.849128127	0.295678544	0.257770339	0.909780136	0.310841547	0.629264594	0.833965125	0.811220622	0.849128127	1.804039271	1.190295679	0.462471569	1.539044731	4.639876496	0.576194886	0.826383624	0	0.500379075	0.363912055	0.227445034	0.644427597
			Dothideales	Dothideaceae	Rachidiicladium	4	1	0	0	0	0	0	0	0	0	0	0	0	0	0	0	0	0	0	0.015163002	0.015163002	0.015163002	0	0	0	0	0	0
					Dothideaceae	8	2	0	0	0	0	0	0	0	0	0	0	0	0	0.007581501	0	0	0	0	0	0	0	0	0	0	0	0	0.053070508	0
					Dothiora	17	2	0.053070508	0.022744503	0.022744503	0	0	0	0	0	0	0	0	0	0	0.030326005	0	0	0	0	0	0	0	0	0	0	0	0	0
				Dothideales	Dothideales	3	1	0	0	0	0	0	0	0	0	0	0	0	0	0.022744503	0	0	0	0	0	0	0	0	0	0	0	0	0	0
				Dothideales_fam_Incertae_sedis	Dothideales_gen_Incertae_sedis	12	4	0	0	0	0	0.015163002	0	0.015163002	0	0	0	0	0	0.060652009	0	0	0	0	0	0	0	0	0	0	0	0	0	0	0
					Homosassia	7	2	0	0	0	0	0	0	0.022744503	0	0	0	0	0	0.015163002	0	0	0	0	0	0	0	0	0	0	0	0	0	0	0
				Neocelosporiaceae	Neocelosporiaceae_gen_Incertae_sedis	4	1	0	0	0	0	0	0.030326005	0	0	0	0	0	0	0	0	0	0	0	0	0	0	0	0	0	0	0	0	0	0
				Saccotheciaceae	Aureobasidium	181573	7	77.32737301	88.46455677	93.29037149	89.84329113	71.16271418	25.54023777	95.37831691	35.28453629	45.58756634	59.89385898	38.94617134	68.10442472	83.5529793	86.27293404	52.78757392	56.39462472	74.87498523	35.66863685	33.23250899	11.42532221	7.854435178	5.577403336	7.640151146	57.79783177	39.04548901	74.12631665
					Kabatiella	2	1	0	0	0	0	0	0	0.015163002	0	0	0	0	0	0	0	0	0	0	0	0	0	0	0	0	0	0	0	0
			Dothideomycetes_ord_Incertae_sedis	Dothideomycetes_fam_Incertae_sedis	Dothideomycetes_gen_Incertae_sedis	19	5	0	0	0	0.007581501	0.022744503	0	0.007581501	0	0	0	0	0.106141016	0	0	0	0	0	0	0	0	0	0	0	0	0	0	0	0
			Myrmecridiales	Hemimyrmecridiaceae	Hemimyrmecridium	7	1	0	0	0.053070508	0	0	0	0	0	0	0	0	0	0	0	0	0	0	0	0	0	0	0	0	0	0	0	0
				Myrmecridiaceae	Ramularia	7	2	0	0	0	0	0	0	0	0	0	0	0	0	0	0	0	0	0.045489007	0	0	0	0	0	0.007581501	0	0	0	0	0
				Teratosphaeriaceae	Constantinomyces	2	1	0	0	0	0	0	0	0	0	0	0	0	0	0.015163002	0	0	0	0	0	0	0	0	0	0	0	0	0	0	0
				Amniculicolaceae	Angustimassarina	22	1	0	0	0	0	0	0	0	0.030326005	0	0	0	0	0	0	0	0.136467024	0	0	0	0	0	0	0	0	0	0	0	0	0
				Cucurbitariaceae	Coniorhytisma	7	2	0	0	0.030326005	0.022744503	0	0	0	0	0	0	0	0	0	0	0	0	0	0	0	0	0	0	0	0	0	0	0	0
					Cryptocoryneaceae	24	1	0	0	0	0	0	0	0	0	0	0	0	0	0	0	0	0.181956027	0	0	0	0	0	0	0	0	0	0	0	0	0
					Neocucurbitaria	10	1	0	0	0	0	0	0	0	0	0	0	0	0	0	0	0	0	0	0	0	0	0	0	0	0	0.007581501	0	0	0	0
				Didymellaceae	Didymellaceae	15	2	0	0	0	0	0	0	0	0	0	0	0	0	0.022744503	0.068223551	0	0	0	0	0	0	0	0.022744503	0	0	0	0	0	0
					Phoma	1404	7	0.129885519	0.128885519	0.022744503	0.181956027	1.271692191	0.045489007	0.318423048	0.068223551	0.030326005	0.068339513	0.341167551	5.579984437	0	0	0.030326005	0.689916605	1.785837756	0.015163002	0	0	0	0	0	0	0	0	0	0
				Didymosphaeriaceae	Didymosphaeriaceae	4	1	0	0	0	0.007581501	0	0.022744503	0	0	0	0	0	0	0	0	0	0	0	0	0	0	0	0	0	0	0	0	0	0
					Kalmusia	4	1	0	0	0	0	0	0	0	0	0	0	0	0	0	0	0	0	0	0.030326005	0	0	0	0	0	0	0	0	0	0
					Paracamarosporium	5	1	0	0	0	0	0	0	0	0	0	0	0	0	0	0	0	0	0	0.037907506	0	0	0	0	0	0	0	0	0	0
					Paraconiothyrium	1	1	0	0	0	0	0	0	0	0	0	0	0	0	0	0	0	0.007581501	0	0	0	0	0	0	0	0	0	0	0	0
					Parasphaeria	12	2	0	0	0	0	0	0	0	0	0	0	0	0	0.015163002	0	0	0	0	0	0	0	0	0	0.007581501	0	0	0	0	0
					Pseudoplagiostoma	18	2	0	0.007581501	0.030326005	0	0	0	0	0	0	0	0.022744503	0.068223551	0	0	0	0	0	0	0	0	0	0	0	0	0.007581501	0	0	0
				Dothidotthiaceae	Dothidotthia	2	1	0	0	0	0	0	0	0	0	0	0	0	0	0	0	0	0	0.007581501	0	0	0	0	0	0	0	0	0	0	0
					Keissleriella	2	1	0	0	0	0	0	0	0	0	0	0	0	0.015163002	0	0	0	0	0	0	0	0	0	0	0	0	0	0	0	0
				Lophiostomataceae	Lophiostomataceae_gen_Incertae_sedis	3	1	0	0	0	0	0	0	0.022744503	0	0	0	0	0	0	0	0	0	0	0	0	0	0	0	0	0	0	0	0	0
					Lophiostomataceae	16	2	0	0	0	0	0	0	0	0	0	0	0	0	0	0	0	0	0	0	0	0.121304018	0	0	0	0	0	0	0	0	0
					Neovaginatispora	5	1	0	0	0	0	0	0	0	0	0	0	0	0	0	0	0	0	0.037907506	0	0	0	0	0	0	0	0	0	0	0
					Massarinaceae	6	1	0	0	0	0	0	0	0	0	0	0	0	0	0	0	0	0	0	0.045489007	0	0	0	0	0	0	0	0	0	0
					Melanommataceae	1	1	0	0	0	0	0	0	0	0	0	0	0	0	0	0	0	0	0	0	0	0	0	0	0	0	0.007581501	0	0	0
					Neoophiosphaeria	3	1	0	0	0.022744503	0	0	0	0	0	0	0	0	0	0	0	0	0	0	0	0	0	0	0	0	0	0	0	0	0
					Paraphaeosphaeria	32	2	0	0	0	0.053070508	0	0	0.007581501	0	0	0	0.068223551	0.007581501	0	0	0	0	0	0.045489007	0	0	0	0	0	0.060652009	0	0	0	0
					Periconia	7	1	0	0	0	0	0	0	0	0	0	0	0	0	0	0	0	0	0	0	0	0.053070508	0	0	0	0	0	0	0	0
				Phaeosphaeriaceae	Acericola	4	2	0	0	0	0	0	0	0	0	0	0	0.015163002	0	0	0	0	0	0	0	0	0	0	0	0.015163002	0	0	0	0	0
					Chaetosphaeronema	12	1	0	0	0	0	0	0	0	0	0	0	0	0	0	0	0	0	0	0.090978014	0	0	0	0	0	0	0	0	0	0
					Paraphoma	12	1	0	0	0	0	0	0	0	0	0	0	0	0	0	0	0	0	0	0.090978014	0	0	0	0	0	0	0	0	0	0
					Phaosphaeria	6	2	0	0	0	0	0	0	0	0	0	0	0	0	0	0	0	0	0	0.045489007	0	0	0	0	0	0	0	0	0	0
					Phaosphaeriaceae_gen_Incertae_sedis	2	1	0	0	0	0	0	0	0.015163002	0	0	0	0	0	0	0	0	0	0	0	0	0	0	0	0	0	0	0	0	0
					Alternaria	1543	8	0.212282032	0.410982563	0.181956027	0.773133116	0.242680036	0.212282032	0.075849389	0.174374526	0.181956027	0.414923563	0.242680036	0.136446702	0.075849311	0.098859515	0.123885519	4.753012213	0.197511963	0.606828091	0.394238859	0.250819938	0.545469082	0	0.060652009	0.507940576	0.166703025	0.121304018
					Bipolaris	4	1	0	0	0	0	0	0	0	0	0	0	0	0	0	0	0	0	0	0.030326005	0	0	0	0	0	0	0	0	0	0
				Pleosporaceae	Camarosporium	12	1	0	0	0	0	0	0	0	0	0	0	0	0	0	0	0	0	0	0.090978014	0	0	0	0	0	0	0	0	0	0
					Pleosporaceae_gen_Incertae_sedis	1	1	0	0	0	0	0	0	0	0	0	0	0	0	0.007581501	0	0	0	0	0	0	0	0	0	0	0	0	0	0	0
					Stemphylium	105	3	0.098559515	0	0	0.136446702	0.060823351	0	0.030326005	0	0	0	0.045489007	0	0	0.007581501	0	0.037907506	0.045489007	0	0.030326005	0	0	0	0.174374526	0.015163002	0.106141016	0
				Pleosporales	Pleosporales	6	3	0	0	0	0	0.015163002	0	0.015163002	0	0	0	0	0	0	0	0	0	0	0	0	0.015163002	0	0	0	0	0	0	0	0
			Pleosporales_fam_Incertae_sedis	Pleosporales_gen_Incertae_sedis	430	5	0.037907506	0.037907506	0.090978014	0.295678544	0.098559515	0	0.068223551	0	0.022744503	0.037907506	1.735161376	0.045489007	0	0	0	0	0	0	0	0.303260045	0	0	0.015163002	0.409401061	0.060652009	0
			Sporormiales	Preussia	16	1	0	0	0	0	0	0	0	0	0	0	0	0	0	0	0	0	0	0	0	0	0	0.121304018	0	0	0	0	0
				Tetraplosphaeriaceae	Tetraplosphaera	1	1	0	0	0	0.007581501	0	0	0	0	0	0	0	0	0	0	0	0	0	0	0	0	0	0	0	0	0	0	0
		Tubeufiales	Tubeufiales	Tubeufiaceae	Bezerromyces	1	1	0	0	0	0	0	0	0	0	0	0	0	0	0	0	0	0	0.007581501	0	0	0	0	0	0	0	0	0
		Venturiales	Sympoventuriaceae	Sympoventuriaceae	Sympoventuriaceae	1	1	0	0	0	0	0	0	0.007581501	0	0	0	0	0	0	0	0	0	0	0	0	0	0	0	0	0	0	0
		Chaetothyriales	Herpotrichiellaceae	Cladophialophora	Cladophialophora	3	1	0	0	0	0	0	0	0.007581501	0	0	0	0	0	0	0	0	0	0	0	0	0	0	0	0	0	0	0	0
					Exophiala	1	1	0	0	0	0	0	0	0	0	0	0	0	0	0	0	0	0	0	0	0	0	0	0	0.007581501	0	0	0	0
		Eurotiomycetes	Eurotiales	Trichocomaceae	Trichocomaceae	5	1	0	0	0	0	0	0	0	0	0	0	0	0	0	0	0	0	0	0	0	0.037907506	0	0	0	0	0	0	0
					Aspergillus	60	6	0	0	0	0	0	0	0	0	0	0	0	0	0	0	0	0	0	0	0	0.098559515	0.318041547	0	0	0.045489007	0	0	0
					Talaromyces	10	1	0	0	0	0	0	0	0	0	0	0	0	0	0	0	0	0	0	0	0	0	0.007581501	0	0	0	0	0	0	0
				Celothelisaceae	Celothelisaceae_fam_Incertae_sedis	20	3	0	0	0	0	0	0	0	0	0	0	0	0	0	0	0	0	0.007581501	0.011722517	0	0	0	0	0	0	0.030326005	0	0
					Minutella	1	1	0	0	0	0	0	0	0	0	0	0	0	0	0	0	0	0	0	0	0	0	0	0	0.007581501	0	0	0	0
				Phaeomelaceae	Xenocellulosporium	5	1	0	0	0	0	0	0	0	0	0	0	0	0	0	0	0	0	0.037907506	0	0	0	0	0	0	0	0	0	0	0
					Phaeomelaceae	3	1	0	0	0	0	0	0	0	0	0	0	0	0	0	0	0	0	0	0	0	0	0	0	0	0.022744503	0	0	0	0
		GS35	GS35_ord_Incertae_sedis	GS35_fam_Incertae_sedis	GS35_gen_Incertae_sedis	4	1	0	0	0	0	0	0	0	0	0	0	0	0	0	0	0	0	0	0	0	0.030326005	0	0	0	0	0	0	0
		Lecanoromycetes	Ostropales	Stictidaceae	Gloniopsis	1	1	0	0	0	0	0	0	0	0	0.007581501	0	0	0	0	0	0	0	0	0	0	0	0	0	0	0	0	0	0
					Schizoxylon	13	3	0	0	0	0	0	0	0.022744503	0	0	0	0.068223551	0	0	0	0	0	0.007581501	0	0	0	0	0	0	0	0	0	0	0
				Erysiphaceae	Blumeria	35	3	0	0.030326005	0.030326005	0.083396513	0	0	0.007581501	0	0	0	0	0.113722517	0	0	0	0	0	0	0	0	0	0	0	0	0	0	0	0
					Erysiphe	1	1	0	0	0	0	0	0	0	0	0	0	0	0	0	0	0	0	0.007581501	0	0	0	0	0	0	0	0	0	0	0
					Golovinomyces	7	2	0	0	0	0.053070508	0	0	0	0	0	0	0	0	0	0	0	0	0	0	0	0	0	0	0	0	0	0	0	0
					Podosphaera	70	2	0.007581501	0.007581501	0.227445034	0.272934041	0	0	0	0	0	0	0	0	0.015163002	0	0	0	0	0	0	0	0	0	0	0	0	0	0	0
				Helotiaceae	Helotiaceae	5	1	0	0	0	0	0	0	0	0	0	0	0	0	0	0	0	0	0	0	0	0.037907506	0	0	0	0	0	0	0	0
				Helotiales	Helotiales	13	1	0	0	0	0	0	0	0	0	0	0	0	0	0	0	0	0	0	0	0	0.098559515	0	0	0	0	0	0	0	0
					Cistella	3	1	0	0	0	0	0	0	0	0	0	0	0	0	0	0	0	0	0	0	0	0.022744503	0	0	0	0	0	0	0	0
				Helotiales_fam_Incertae_sedis	Cryptodiscus	2	1	0	0	0	0	0	0	0.015163002	0	0	0	0	0	0	0	0	0	0	0	0	0	0	0	0	0	0	0	0	0
					Hamiphospora	2	1	0	0	0	0	0	0	0	0	0	0	0	0	0	0	0	0	0	0	0	0.015163002	0	0	0	0	0	0	0	0
					Phacidiella	1	1	0	0	0	0	0	0	0	0	0	0	0	0	0	0	0	0	0	0.007581501	0	0	0	0	0	0	0	0	0	0
					Tomasellia	5	2	0	0	0	0	0	0	0	0	0	0	0	0	0	0	0	0	0	0.015163002	0	0.037907506	0	0	0	0	0	0	0	0
					Lachnaceae_gen_Incertae_sedis	13	1	0	0	0	0	0	0	0	0	0	0	0	0	0.098559515	0	0	0	0	0	0	0	0	0	0	0	0	0	0	0
				Lachnaceae	Mollisia	3	2	0	0	0	0	0	0	0	0	0	0	0	0	0.007581501	0	0	0	0.015163002	0	0	0	0	0	0	0	0	0	0	0
					Pirottaella	2	1	0	0	0	0	0	0	0	0	0	0	0	0	0	0	0	0	0	0.015163002	0	0	0	0	0	0	0	0	0	0
				Sclerotiniaceae	Botrytis	16600	1	0	0	0	0	0	0	0	0	0	0	0	0	0	0	0	0	8.946173142	0.459727046	16.6489765	0.113722517	16.49734647	0.561031084	82.63878989	0	0	0	0.051634002
					Pyrenopeziza	10958	1	0	0	0	0	0	0	0	0	0.144048522	0.250189538	4.238859156	0.022744503	0	0	0	0	14.76118273	0	0	0	0	0	0	0.523125578	63.13874147	0	0	0
					Sclerotinia	1	1	0	0	0	0	0	0	0	0	0	0	0	0	0	0	0	0	0	0.007581501	0	0	0	0	0	0	0	0	0	0
					Sclerotiniaceae	31045	10	0	0	0	0	0	0	0	29.09780136	0	0	0	0	0	0	0	0	0	0.075815011	0.075805661	0	74.25334463	38.48778476	84.49583017	0	0	0	0	0
				Trichalosiaceae	Trichalosim	3	1	0	0	0	0	0	0	0	0	0	0	0	0	0	0	0	0	0.022744503	0	0	0	0	0	0	0	0	0	0	0
					Callophoria	325	1	0	0	0	0	0	0	0	0	0	0	0	0	0	0	0	0	0	2.463398787	0	0	0	0	0	0	0	0	0	0
				Tympanidaceae	Pallidophorina	9557	3	1.971190296	0.030326005	0.075815011	0.128885519	0.098559515	0.045489007	0.144048522	8.536770281	0.772554966	13.55572403	4.689552691	0.477634572	0.272934041	1.51146323	2.416498863	3.78832207	0	0.068223551	1.205458681	1.736165376	0.879454132	0	0	20.76573161	0.333586505	0	0
					Tympanis	2	1	0	0	0	0	0	0	0	0	0	0	0	0	0	0	0	0	0	0	0	0	0	0	0	0	0.015163002	0	0
			Lecanoromycetes_ord_Incertae_sedis	Lecanoromycetes_fam_Incertae_sedis	Lecanoromycetes_gen_Incertae_sedis	92	1	0	0	0	0	0	0	0	0	0	0	0	0	0	0	0	0	0.007581501	0	0	0	0	0	0	0	0	0	0	0
					Lecanoromycetes	7	1	0	0	0	0	0	0	0	0	0	0	0	0	0	0	0	0	0	0.689916603	0	0	0	0	0	0	0	0	0	0
					Pseudeurotiaceae_gen_Incertae_sedis	12	1	0	0	0	0	0	0	0	0	0	0	0	0	0	0	0	0	0	0.037907506	0	0	0	0	0	0	0	0	0	0
				Pseudeurotiaceae	Pseudeurotium	15	1	0	0	0	0	0	0	0	0	0	0	0	0	0	0	0	0	0.007581501	0.083396513	0	0	0	0	0	0	0.113722517	0	0	0
					Pseudogymnoascus	8	1	0	0	0	0	0	0	0	0	0	0	0	0	0	0	0	0	0	0	0	0	0	0	0	0	0.060652009	0	0	0	0
				Thelebolaceae	Thelebolaceae	17	1	0	0	0	0	0	0	0	0	0	0	0	0	0	0	0	0	0	0	0	0	0	0	0

Baltazar et al., Phytopathology

Supp1ementary Tabela S4 - Results of DESeq analysis at genus level in wood samples, with and without the presence of *Monilinia fruticola.*

	baseMean	log2FoldChange	lfcSE	stat	pvalue	padj
Pycnopeziza	194,6079143	24,56933324	2,51550179	9,767169851	1,56E-22	2,49E-21
Diaporthe	71,03042083	-26,01735196	2,964970387	-8,774911237	1,71E-18	1,37E-17
Unknown	15876,91495	-2,720650963	0,770082042	-3,53293651	0,000410971	0,002191846
Botrytis	612,9377792	-6,996102431	2,322648549	-3,012122705	0,002594277	0,010377108
Pallidophorina	936,8633584	2,579511393	1,207286244	2,136619552	0,032628948	0,104412634
Alternaria	129,8119655	1,174618887	0,711581248	1,65071647	0,098796483	0,260659523
Tremellales_gen_Incertae_sedis	82,6108586	2,110773857	1,335680545	1,580298421	0,114038541	0,260659523
Phoma	26,93748152	-2,44253283	1,732227338	-1,410053274	0,158523953	0,304970421
Taphrina	6,70564743	-2,512544085	1,837657822	-1,367253498	0,171545862	0,304970421
Cytospora	0,953996224	-3,741506304	2,991952252	-1,2505234	0,211108413	0,33777346
Vishniacozyma	1344,459488	0,358613893	0,346976515	1,033539383	0,30135155	0,438329527
Pleosporales_gen_Incertae_sedis	42,73316752	2,18220034	2,33990313	0,932602855	0,351025059	0,468033412
Cladosporium	282,2943813	-0,53475161	0,641779034	-0,833233219	0,404713211	0,479917686
Fungi_gen_Incertae_sedis	105,4766872	0,977637311	1,212128083	0,806546209	0,419927975	0,479917686
Tremellomycetes_gen_Incertae_sedis	126,0731305	1,380854846	1,945365054	0,709817853	0,477817097	0,50967157
Aureobasidium	14519,67357	0,041056433	0,428831007	0,095740356	0,923726788	0,923726788

Baltazar et al., Phytopathology

Supp1ementary Tabela S5 - Results of DESeq analysis at genus level in flower samples, with and without the presence of *Monilinia fruticola.*

	baseMean	log2FoldChange	lfcSE	stat	pvalue	padj
Taphrina	231,6565147	10,44870256	2,703851448	3,864377447	0,000111373	0,001113729
Aureobasidium	24484,94755	-1,560361761	0,625324815	-2,495282009	0,012585706	0,06292853
Phoma	74,78045318	1,661067756	0,779127454	2,131958958	0,033010221	0,110034069
Alternaria	96,38690483	-1,497163563	0,743498466	-2,013674046	0,044043767	0,110109417
Cladosporium	124,8458857	0,644552086	1,234630383	0,522060768	0,601628021	0,9256816
Pallidophorina	41,16985077	0,21820771	0,996447216	0,218985719	0,826661172	0,9256816
Filobasidium	60,77788426	0,108789577	0,8587414	0,12668491	0,89918979	0,9256816
Vishniacozyma	2322,892326	0,022786197	0,244278996	0,093279396	0,9256816	0,9256816
Tremellomycetes_gen_Incertae_sedis	125,4844265	0,680066102	1,681457912	0,404450267	0,685881642	0,9256816
Unknown	497,3558013	0,851193046	1,172306434	0,726084086	0,467787224	0,9256816
Diaporthe	307,4889171	-25,77002114	3,58317675	-7,19194808	NA	NA
Tremellales_gen_Incertae_sedis	119,513289	9,493800693	3,907000853	2,429945897	NA	NA
Fungi_gen_Incertae_sedis	144,8965751	7,159949099	2,091223306	3,423808963	NA	NA

Supp1ementary Tabela S6 - Results of statistical tests for normality, variance homogeneity, and significance for diversity indices (Chao1, Shannon, and Simpson) in wood and flower samples, with and without the presence of *Monilinia fruticola*

Test/Index	Wood Samples	Flowers Samples	Wood vs. Flowers Samples (*Monilinia* Detected)	Wood vs. Flowers Samples (*Monilinia* Not Detected)
Chao1 Index (Normality)	Shapiro-Wilk: W = 0.76519, p = 0.00027 (non-normal)	Shapiro-Wilk: W = 0.86301, p = 0.1997 (normal)	Shapiro-Wilk: W = 0.86495, p = 0.03566 (non-normal)	Shapiro-Wilk: W = 0.79568, p = 0.00837 (non-normal)
Chao1 Index (Variance Homogeneity)	Levene's test: F = 2.8142, p = 0.1107 (homogeneous)	Levene's test: F = 0.4609, p = 0.5345 (homogeneous)	Variances: p > 0.19 (homogeneous across materials)	Variances: p = 0.3697 (homogeneous)
Chao1 Index (Significance Test)	Wilcoxon: W = 70, p = 0.1284 (no significant difference)	t-test: t = -4.7336, p = 0.00908 (significant difference)	Wilcoxon: W = 33, p = 0.01263 (significant difference, flowers have higher richness)	Wilcoxon: W = 12, p = 0.8531 (no significant difference)
Shannon Index (Normality)	p > 0.05 (near-normal)	p > 0.05 (normal)	p > 0.05 (normal)	p = 0.02145 (approx. normal)
Shannon Index (Variance Homogeneity)	p = 0.9895 (homogeneous)	p > 0.79 (homogeneous)	Variances: p > 0.19 (homogeneous)	Variances: p > 0.53 (homogeneous)
Shannon Index (Significance Test)	t-test: t = -0.9886, p = 0.336 (no significant difference)	t-test: t = -3.2557, p = 0.03121 (significant difference)	t-test: t = -0.68227, p = 0.508 (no significant difference)	W = 2, p = 0.03636 (significant difference, flowers more diverse)
Simpson Index (Normality)	p > 0.05 (near-normal)	p > 0.05 (normal)	p > 0.05 (normal)	p = 0.05723 (approx. normal)
Simpson Index (Variance Homogeneity)	p = 0.6268 (homogeneous)	p > 0.79 (homogeneous)	Variances: p > 0.19 (homogeneous)	Variances: p > 0.53 (homogeneous)
Simpson Index (Significance Test)	t-test: t = -2.1065, p = 0.04946 (significant difference, higher dominance in detected group)	t-test: t = -2.9744, p = 0.04097 (significant difference, higher dominance in detected group)	t-test: t = -1.9231, p = 0.07851 (approaching significance, potential difference in dominance)	p = 0.07115 (approaching significance)

Baltazar et al., Phytopathology

Supp1ementary Table S7 - Alpha diversity indexes for each

Samples	Observed	Chao1	se.chao1	ACE	se.ACE	Shannon	Simpson	InvSimpson	Fisher
EB.144	21	24	4,57233529	22,3877551	2,156745165	0,559194461	0,214108202	1,272439797	2,443585711
EB.145	23	23	0	23	2,377430107	0,363405584	0,128419513	1,147340968	2,708776721
EB.148	36	37,2	1,838311521	37,68585261	2,89458959	0,81848318	0,332698928	1,498573945	4,51065046
EB.149	47	49	2,583305903	49,47621478	3,466148713	1,167763588	0,473254441	1,898449799	6,123323928
EB.150	52	54,15384615	2,267560452	58,37057611	3,835404987	0,950346243	0,360407769	1,563496164	6,87897813
EB.161	49	49,85714286	1,394189327	50,88222325	3,454836275	1,368167905	0,524631464	2,103631023	6,423989876
EB.144	18	19	2,299885581	19,3222872	1,784097149	0,949733363	0,391201113	1,642578562	2,052892727
EB.149	14	14	0,481812056	14,28103191	1,85408835	0,892768534	0,485597642	1,944003532	1,546762542
EB.153	16	16	0	16	1,854049622	1,647003208	0,757213456	4,118844417	1,797568852
EB.155	21	21	0,487950036	21,3	1,965831409	1,592297764	0,714115031	3,497910375	2,443585711
EB.157	20	20	0	20	1,936491673	1,316021681	0,594067116	2,463461424	2,31237699
EB.160	23	23	0	23	2,284160963	1,591958207	0,710246155	3,451205275	2,708776721
EB.6670	31	31,5	1,292146608	32,04995748	2,564305388	0,814642871	0,297319252	1,423121387	3,802867918
EB.6678	18	21	4,559135256	20,18641869	2,199598498	0,756461714	0,339523452	1,5140583	2,052892727
EB.6679	11	11	0	11	1,279204298	1,112088692	0,587102665	2,421909554	1,18003522
EB.6681	25	25	0,489897949	25,21562735	2,280592116	1,464459565	0,626872806	2,680051243	2,977481674
EB.749	25	27,5	3,153281119	30,11772853	2,835712162	1,008080038	0,424816282	1,738574944	2,977481674
EB.754	38	41,33333333	4,118373054	41,23644779	3,145845774	1,948098374	0,792510902	4,819530334	4,798410475
EB.756	37	38,5	2,228113246	40,40480691	3,031025236	1,840571464	0,766110736	4,275527583	4,654210678
EB.758	30	30,2	0,620074766	31,13173382	2,689551985	1,024254954	0,437153804	1,776684302	3,663409299
EB.762	84	84,85714286	1,394683514	85,15186696	4,406801807	2,076406487	0,786036243	4,673688729	11,99357418
EB.764	56	56	0,247757802	56,20896666	3,682481958	0,917827862	0,305103885	1,439064025	7,492805742
EB.774	16	17	1,806849712	19,0310775	2,108469642	0,68613393	0,306720015	1,442418679	1,797568852
EB.777	28	28,6	1,183821003	30,3820957	2,779705964	1,229844588	0,597705604	2,485741812	3,386711583
EB.779	22	22,25	0,733879898	23,12214938	2,38060843	0,935371451	0,509197056	2,037477593	2,575728713
EB.782	17	17	0,161690417	17,32525952	2,029897306	0,833396132	0,419782142	1,72349056	1,924690166

Baltazar et al., Phytopathology

Supp1ementary Tabela S8 - Results of DESeq analysis of FungalTraits results in wood samples, with and without the presence of *Monilinia fruticola.*

FulgalTraits	baseMean	log2FoldChange	lfcSE	stat	pvalue	padj
dung_saprotroph	3,776601809	-21,87260283	2,970090726	-7,364287776	1,78E-13	2,32E-12
plant_pathogen	1112,252205	-2,857483425	0,641213895	-4,456365415	8,34E-06	5,42E-05
litter_saprotroph	508,8127823	1,900591011	0,767939522	2,474922774	0,013326499	0,057748162
nectar/tap_saprotroph	4,556729217	-5,678222124	2,967268401	-1,913619315	0,055668815	0,146751223
NA	13024,87184	-1,399224039	0,733499239	-1,907601215	0,056442778	0,146751223
mycoparasite	62,62684112	-2,057908204	1,257354101	-1,636697412	0,10169371	0,203868192
unspecified_saprotroph	39,28106944	-1,960343165	1,225823975	-1,599204458	0,10977518	0,203868192
sooty_mold	13658,28027	0,637987396	0,431610103	1,478156772	0,139365821	0,22646946
wood_saprotroph	34,5768612	-1,97131996	1,912922891	-1,030527665	0,302762372	0,437323427
foliar_endophyte	0,340271703	-2,113635851	3,007488991	-0,702790885	0,482186078	0,626841902
lichenized	0,115824897	1,255509437	3,029574457	0,414417752	0,67856819	0,735115539
soil_saprotroph	1570,340957	0,194386191	0,418939782	0,463995542	0,642650939	0,735115539
epiphyte	1,739558522	0,650514017	2,384933425	0,272759822	0,785037846	0,785037846
animal_parasite	0	0	0	0	1	NA

Supp1ementary Tabela S9 - Results of DESeq analysis of FungalTraits results in flower samples, with and without the presence of *Monilinia fruticola.*

	baseMean	log2FoldChange	lfcSE	stat	pvalue	padj
sooty_mold	21471,09612	-1,355982913	0,629934727	-2,152576853	0,031351949	0,313519493
NA	861,0354369	1,194151033	0,664134534	1,798055923	0,072168146	0,36084073
mycoparasite	18,3950069	-1,897057204	1,268521944	-1,495486312	0,13478757	0,449291899
epiphyte	1,250078418	2,987813533	3,918319436	0,762524235	0,445747184	0,742911974
nectar/tap_saprotroph	0,529463796	-3,593026108	4,015518912	-0,894785004	0,370902028	0,742911974
unspecified_saprotroph	98,54255043	0,719102024	0,893412849	0,804893309	0,42088125	0,742911974
plant_pathogen	602,252994	-0,486080755	0,780344904	-0,622905017	0,533346941	0,761924202
litter_saprotroph	115,3165875	0,182553983	0,692017901	0,26379951	0,791934412	0,910720461
soil_saprotroph	2246,951515	-0,067645995	0,603282739	-0,112129836	0,910720461	0,910720461
wood_saprotroph	5,460004682	-0,333871394	1,625600646	-0,205383404	0,837272586	0,910720461

Supplementary Table S10 – Identification of fungal isolates recovered from sampled orchards and the corresponding accession numbers

Orchard	Isolate	Identification	Similarity with NCBI database	Reference NCBI	NCBI Acession Number
P1	144	*Diaporthe amygdali*	100%	OL943982.1	PQ584233
	144C	*Alternaria sp.*	100%	OP703616.1	PQ584234
P2	148A	*Cladosporium sp.*	100%	MN275871.1	PQ584235
	148B	*Alternaria alternata*	100%	MT556702.1	PQ584236
P3	149A	*Cyospora leucostoma*	99%	KY977535.1	PQ584237
	149B	*Botryosphaeria dothidea*	100%	MF398856.1	PQ584238
	149C	*Botryosphaeria dothidea*	99,77%	MK982836.1	PQ584239
	149D	*Botryosphaeria dothidea*	99,77%	MK982836.1	PQ584240
	153A	*Alternaria alternata*	100%	KU366278.1	PQ584241
	155A	*Alternaria alternata*	100%	KU366278.1	PQ584242
	155B	*Alternaria alternata*	99,63%	MT446184.1	PQ584243
	775A	*Botrytis cinerea*	100%	MH860108.1	PQ584281
	775B	*Alternaria arborescens*	100,00%	KM246282.1	PQ584282
P4	157	*Alternaria sp.*	100%	OP703616.1	PQ584244
	160A	*Epicoccum nigrum*	99,81%	MT556704.1	PQ584245
	160B	*Sordaria fimicola*	99,83%	MK432735.1	PQ584246
	160C	*Sordaria fimicola*	100%	MK432735.1	PQ584247
	160D	*Alternaria arborescens*	99,82%	KX768144.1	PQ584248
	160E	*Monilinia fructicola*	99,61%	MH864497.1	PQ584249
	161A	*Alternaria sp.*	100%	OP703616.1	PQ584250
	161B	*Epicoccum nigrum*	100%	KT898578.1	PQ584251
	161C	*Alternaria sp.*	100%	OQ064057.1	PQ584252
	161D	*Diaporthe ambigua*	99,81%	MZ066749.1	PQ584253
	161E	*Monilinia fructicola*	100%	MT804333.1	PQ584254
	161F	*Alternaria alternata*	100%	MT556702.1	PQ584255
	161G	*Monilinia fructicola*	99,80%	MH127836.1	PQ584256
	161H	*Alternaria sp.*	100%	OP703616.1	PQ584257
	161I	*Alternaria alternata*	100%	MN944587.1	PQ584258
	779A	*Cytospora sorbicola*	100%	OR036895.1	PQ584283
	779B	*Monilinia fructicola*	100%	MT804333.1	PQ584284
P5	753A	*Alternaria sp.*	100%	OP703616.1	PQ584263
	753B	*Diaporthe amygdali*	100%	MH205921.1	PQ584264
P6	754A	*Cytospora leucostoma*	99,83%	MT318593.1	PQ584265
	754B	*Monilinia fructicola*	99,62%	MT804333.1	PQ584266
P7	756A	*Diaporthe amygdali*	99,64%	MH205921.1	PQ584268
	756C	*Alternaria arborescens*	99,82%	KX768144.1	PQ584269
P8	758A	*Alternaria sp.*	100%	MT089982.1	PQ584270
	758B	*Alternaria alternata*	100%	MT556702.1	PQ584271
P9	762	*Diaporthe amygdali*	99,82%	MH205921.1	PQ584272
P10	764A	*Alternaria alternata*	99,82%	MN944587.1	PQ584273
	765B	*Sordaria fimicola*	99,20%	MK432735.1	PQ584274
	766D	*Alternaria alternata*	100%	KU182490.1	PQ584275
P11	774	*Botrytis cinerea*	100%	MH860108.1	PQ584280
	782	*Alternaria sp.*	99,25%	KU556507.1	PQ584290